2023-04-20

Rigorous Computation of the Evans Function

Devin McGhie
Brigham Young University

Rigorous Computation of the Evans Function

Devin McGhie

A dissertation submitted to the faculty of
Brigham Young University
in partial fulfillment of the requirements for the degree of

Doctor of Philosophy

Blake Barker, Chair
Mark Allen
Lennard Bakker
Jared Whitehead

Department of Mathematics

Brigham Young University

ABSTRACT

Rigorous Computation of the Evans Function

Devin McGhie
Department of Mathematics, BYU
Doctor of Philosophy

We develop computer-assisted methods of proof for rigorous computation of the Evans function in order to prove stability of traveling waves. We use the parameterization method, series solutions, and the Newton-Kantorovich Theorem to obtain precise, rigorous error bounds for the numerical solution of the ODE used in the construction of the Evans function. We demonstrate these methods on a scalar reaction-diffusion model and on the Gray-Scott model.

Keywords: Evans function, rigorous computation, stability of waves, Gray-Scott model

Acknowledgements

I am very grateful to my dissertation advisor, Blake Barker, for the many hours of time, help, and motivation he has provided me with and for his willingness to help me out multiple times a week and help determine the direction to go for the research.

I am also very grateful to my parents, Brian and Susan McGhie, for their constant concern and care for my schooling and research. I also am thankful for them teaching me the love of math early on.

I also appreciate my committee members, Professors Mark Allen, Lennard Bakker, and Jared Whitehead, for being willing to participate and spend time helping with my work. I would like to thank J.D. Mireles James and Christian Reinhardt for useful discussions. Also I appreciate the graduate committee for their trust by admitting me and to the department for financial support. I also thank Lonette Stoddard and Debi Tait and other mathematics department staff for their help and guidance through the process. I also appreciate the many past professors I have had for their wonderful inspiration and guidance through the program.

Contents

List of Tables

List of Figures

Chapter 1. Introduction

Many physical processes can be modeled well with partial differential equations. Traveling wave solutions play an especially important role in PDE models of fluid flow and chemical reactions. Of particular interest is determining the stability of traveling wave solutions. A wave is stable if small perturbations of the wave do not significantly alter the long term behavior of the PDE solution. If a wave is not stable, then a small perturbation of the wave may result in the long term behavior of the solution varying drastically. This can have significant implications. For example, an unstable wave may not even be observed in nature since noise is always present in the physical system. Alternatively, if the model predicts a stable wave, one expects a corresponding wave to exist in the physical phenomena.

Much work has been done studying the stability of traveling wave solutions of PDEs. In the last several decades, huge strides have been made concerning the theory of stability of nonlinear waves. For a very large class of systems, stability of a wave is implied by spectral stability of the wave. Determining spectral stability of a traveling wave solution reduces to determining the spectrum of an ODE eigenvalue problem. Typically, this ODE is too complicated to obtain an explicit solution, and so one uses numerical methods to approximate the solution to the ODE. By obtaining rigorous error bounds on the ODE solutions, including using an interval arithmetic package to bound rounding error that occurs during the computation, one may be able to prove the spectrum lies in the stability region.

The main challenge we address in this dissertation is how to rigorously compute the Evans function, a complex analytic function whose zeros correspond to eigenvalues of the ODE eigenvalue problem obtained from linearizing the governing equations about the traveling wave. The wave is said to be spectrally stable if these eigenvalues, with the exception of the zero eigenvalue corresponding to translational invariance, have negative real part. The wave is said to be asymptotically orbitally stable if any sufficiently small perturbation of the wave converges to a spatial translate of the wave. Spectral stability implies asymptotic orbital

stability for all the systems we consider in this dissertation, and for a very broad class of problems; for details see [12, 15, 16, 18, 21, 28, 29, 34, 41, 42]. Thus, to prove nonlinear-orbital stability, one may prove that the Evans function has no zeros in the closure of the right half of the complex plane, with the exception of the origin.

Usually one must resort to numerical methods to approximate the Evans function, which provides compelling evidence of stability, but does not constitute a proof. In this dissertation we develop a computer assisted method of proof, or CAMP, to prove spectral stability, hence nonlinear-orbital stability, of traveling waves in physical systems. A detailed description of CAMP is given, for example, in [8, 13, 31, 38]. **CAMP** consists of rigorous analysis assisted at strategic times by rigorous computations. By a rigorous computation, we mean a computation that provides a rigorous error bound on numerical rounding error. We use the MATLAB based package INTLAB [33], which is a well-developed interval arithmetic package. INTLAB rigorously bounds rounding error by computing with appropriate rounding a machine representable lower and upper bound on a quantity, that is an interval containing the desired quantity.

We note that CAMP have been used to prove several notable results, including proving Mitchell Feigenbaum's universality conjecture in non-linear dynamics, the Kepler conjecture, and Warwick Tucker's proof of the existence of the Lorenz attractor (14th of Smale's problems).

There are a few results in the literature in which stability of waves is proven using rigorous computation; see for example [2, 3, 5]. We note the recent result described in [7], which describes an extremely efficient method for validated numerics for systems of a certain form. There are many systems of interest for which this method does not apply. For these, the Evans function is a useful tool for proving stability. In this dissertation, we develop a general approach for proving stability of waves using rigorous computation of the Evans function. We begin by providing more background about the Evans function.

Chapter 2. Mathematical background

In this chapter we provide details about the theoretical tools we use. We begin by discussing stability of traveling waves. We describe the Evans function, an analytic function whose zeros correspond in location and multiplicity to the eigenvalues of an ODE eigenvalue problem one obtains by linearizing the nonlinear PDE equations about a traveling wave solution. When these eigenvalues, except for certain eigenvalues at the origin, lie in the left half plane, the wave is said to be spectrally stable. For a large class of PDEs, spectral stability implies nonlinear stability.

We also provide details about useful theory we use in developing computer assisted methods of proof (CAMP) for establishing stability of traveling wave solutions. We review results regarding error bounds when interpolating analytic functions, and results that say the uniform limit of analytic functions is analytic. We review bounds on the modulus of ODE solutions, and we review the Newton-Kantorovich contraction mapping principle, a main tool used in our CAMP.

2.1 Stability of Traveling Waves

We consider evolution equations of the form

$$u_t + f(u)_x = (B(u)u_x)_x + (C(u)u_{xx})_x, \tag{2.1}$$

where the spatial variable $x \in \mathbb{R}$, the time variable $t \in \mathbb{R}$, the unknown dependent variable $u : \mathbb{R}^2 \to \mathbb{R}^n$, the flux term f is a function $f : \mathbb{R}^n \to \mathbb{R}^n$, and the diffusion matrix B and the dispersion matrix C are sufficiently smooth functions

$$B : \mathbb{R}^n \to \mathbb{R}^{n\times n}, \quad C : \mathbb{R}^n \to \mathbb{R}^{n\times n}.$$

We specifically consider traveling waving solutions which are solutions of the PDE that are stationary in a co-moving frame as described in the following definition.

Definition 1. A solution of (2.1) that takes the form

$$u(x,t) = \check{u}(x - ct)$$

is called a traveling wave solution, where $c \in \mathbb{R}$ is the wave speed. We refer to $\check{u}$ as the traveling wave profile.

Looking for a traveling wave solution with wave speed c is equivalent, via the transformation $x \to x - ct$, to looking for a stationary solution of

$$u_t + (f'(u) - c)u_x = (B(u)u_x)_x + (C(u)u_{xx})_x.$$

We only consider the case that the wave profile is smooth with asymptotically constant end-states,

$$\lim_{x\to\pm\infty} \check{u}(x) = u_\pm, \quad \lim_{x\to\pm\infty} \check{u}^{(n)}(x) = 0, \quad n \geq 1.$$

In the above equation, the superscript (n) denotes the n-th derivative with respect to x.

We are interested in determining the stability of these waves. Our main objective in this dissertation is to develop computer assisted methods of proof (CAMP) for proving stability of traveling wave solutions of PDEs of the form given in (2.1). As part of proving stability, we must obtain an approximation of the traveling wave profile with concrete error bounds on the approximation error. The method we use to do this proves existence of the profile as well. We now describe what we mean by stability.

Definition 2. A solution U is asymptotically orbitally stable with respect to $\mathbb{P}$, the set of acceptable permutations, if for all $V \in \mathbb{P}$,

$$U(x,t) = \check{U}(x) + V(x,t) \to \check{U}(x + \epsilon) \tag{2.2}$$

for some $\epsilon \in \mathbb{R}$ as $t \to \infty$.

Thus, a wave is stable if a sufficiently small perturbation of the wave converges to a spatial translate of the unperturbed wave as time tends to infinity. Determining the nonlinear orbital stability of a wave requires understanding the spectrum of the wave. Spectral stability, which we introduce next, plays a central role in determining stability; see [19, 27, 28, 42].

2.1.1 Spectral Stability. By linearizing (2.1) about the standing wave $\check{U}$, and then looking for separated solutions, we obtain the eigenvalue problem,

$$\lambda V = LV := -(\alpha(\check{U}) \cdot V))_x + (\beta(\check{U}) \cdot V_x)_x - (\gamma(\check{U}) \cdot V_{xx})_x \tag{2.3}$$

where $\alpha(\check{U}) \cdot V = dg(\check{U}) \cdot V - d\beta(\check{U}) \cdot V \cdot \check{U}_x - d\gamma(\check{U}) \cdot V \cdot \check{U}_{xx}$.

We are interested in the spectrum of L, which we now define.

Definition 3. We define:

- The spectrum $\sigma(L)$ of L is the set of all $\lambda \in \mathbb{C}$ such that $L - \lambda I$ is not invertible.
- The point spectrum $\sigma_p(L)$ of L is the set of all isolated eigenvalues of L with finite multiplicity.
- The essential spectrum $\sigma_e(L)$ of L is the entire spectrum not including the point spectrum, i.e. $\sigma_e(L) = \sigma(L) \setminus \sigma_p(L)$.

With the spectrum of a wave defined, we can now define what we mean by spectral stability of a traveling wave.

Definition 4. A wave is spectrally stable if there is no spectrum of the eigenvalue problem (2.3) in the deleted right half plane: $\mathbb{C}_+ := \{\lambda \in \mathbb{C} \setminus \{0\} | Re(\lambda) \geq 0\}$.

For a wide class of systems, spectral stability implies nonlinear orbital stability; see [14, 19, 25, 26, 28, 27, 30, 36, 42].

We note that $\sigma_p(L) \neq \emptyset$ since 0 is always an eigenvalue corresponding to translational invariance, as described in the following result of Sattinger.

Lemma 5. *(Sattinger [35]) The derivative of the profile $\check{U}'$ is an eigenfunction of L with eigenvalue* 0.

Proof. By translational invariance, we have $\forall \delta \in \mathbb{R}$ that

$$F(\check{U}(x + \delta)) = 0,$$

where

$$F(u) := -(f'(u) - c)u_x + (B(u)u_x)_x + (C(u)u_{xx})_x.$$

Taking the derivative with respect to δ and setting $\delta = 0$, we obtain

$$0 = \frac{\partial}{\partial \delta} F(\check{U}(x+\delta))|_{\delta=0} = F'(\check{U}(x))\check{U}'(x) = L(\check{U}'(x)).$$

□

The main focus of this dissertation is developing computer assisted methods of proof to obtain rigorous error bounds on numerical computations of the Evans function in order to determine if a wave is spectrally stable. We must also verify for given systems that the essential spectrum is well-behaved in order to prove a wave is stable. Fortunately, this is straightforward due to the work of Henry, as we now describe.

2.1.2 Essential Spectrum. Recall the following result of Henry regarding essential spectrum.

Theorem 6. *(Henry [18])*
The essential spectrum of L in (2.3) is sharply bounded to the right of $\sigma_e(L_+) \cup \sigma_e(L_-)$, where $L_\pm$ correspond to the operators obtained by linearizing about the constant solutions $\check{U} = U_\pm$, respectively.

Thus, the essential spectrum is determined by solving the eigenvalue problem,

$$\lambda V = LV := -\alpha_\pm V_x + \beta_\pm V_{xx} - \gamma_\pm V_{xxx}, \tag{2.4}$$

where $\alpha_\pm := dg(U_\pm)$, $\beta_\pm := \beta(U_\pm)$, and $\gamma_\pm := \gamma(U_\pm)$.
We note that the linear operators $L_\pm$ have no point spectrum, so $\sigma(L_\pm) = \sigma_e(L_\pm)$.

To solve the eigenvalue problem which gives the essential spectrum, we use the Fourier transform,

$$\widehat{(L - \lambda I)}^{-1} V = (-i\zeta\alpha_\pm - \zeta^2\beta_\pm + i\zeta^3\gamma_\pm - \lambda I)^{-1} V, \ \ \zeta \in \mathbb{R}. \tag{2.5}$$

Then we can see that $L - \lambda I$ is singular whenever $0 \in \sigma(-i\zeta\alpha_\pm - \zeta^2\beta_\pm + i\zeta^3\gamma_\pm - \lambda I)$. Another way of saying this is this equivalence:

$$\lambda \in \sigma(L_\pm) \iff \lambda \in \sigma(-i\zeta\alpha_\pm - \zeta^2\beta_\pm + i\zeta^3\gamma_\pm - \lambda I) \tag{2.6}$$

for some $\zeta \in \mathbb{R}$. We thus have $2n$-curves $\lambda_n^\pm$ which correspond to

$$\sigma(-i\zeta\alpha_\pm - \zeta^2\beta_\pm + i\zeta^3\gamma_\pm - \lambda I).$$

2.2 Theoretical Background of the Evans Function

In this section we describe the background needed to prove spectral stability of a traveling wave, hence nonlinear orbital stability. By a traveling-wave solution of $U_t = F(U)$ where F is a differential operator in x, we mean a solution of the form

$$U(x,t) = \check{U}(x - ct),$$

where c is wave speed. Changing to co-moving coordinates $x \to x - ct$ and linearizing about the (now stationary) profile $\check{U}$, we obtain the eigenvalue problem,

$$\lambda V = LV := (DF(\check{U}) + c\partial_x)V, \tag{2.7}$$

where $\lambda \in \mathbb{C}$. We say the traveling wave profile $\check{U}$ is spectrally (orbitally) stable if first, L has no spectrum in $P = \{\lambda \in \mathbb{C} | \Re(\lambda) \geq 0\} \backslash \{0\}$ and second, multiplicity of spectra at $\lambda = 0$ (always present by translational invariance), appropriately defined, corresponds to the dimension of the manifold of nearby traveling-wave solutions. Spectral stability has been shown (for example see [12, 15, 16, 18, 21, 28, 29, 34, 41, 42]) in a variety of contexts, to determine nonlinear orbital stability of traveling-wave solutions.

One may determine the presence of unstable eigenvalues of (2.7) when $\check{U}$ is a viscous shock wave by constructing the Evans function, $D(\lambda)$, which consists of writing (2.7) as a first order ODE,

$$W'(x) = A(x,\lambda)W(x), \quad A_{\pm}(\lambda) := \lim_{x\to\pm\infty} A(x;\lambda), \tag{2.8}$$

and then taking the Wronskian at $x = 0$ of the linearly independent spanning set of ODE solutions W_1, ...,W_k that span the unstable manifold at $x = -\infty$ and the linearly independent spanning set of solutions W_{k+1},...,W_n that span the stable manifold at $x = +\infty$, where n is the dimension of the ODE system. The zeros of the Evans function, $D(\lambda) = \det[W_1, ..., W_k, W_{k+1}, ..., W_n]|_{x=0}$, correspond in location and multiplicity to the eigenvalues of (2.7). With initializing basis chosen appropriately at $x = \pm\infty$, the Evans function is analytic in λ. Consequently, the existence or absence of eigenvalues of (2.7) may be determined by computing the Evans function on appropriately chosen contours and counting the winding number of the image.

For many systems, an explicit representation of the Evans function is not known and so numerical approximation is used. Computing the Evans function numerically can be challenging due to competing growth modes in the solutions of (2.8) leading to loss of significance. Thus numerical methods must be chosen carefully. Many algorithms have been developed for computing the Evans function (for a few examples see [4, 20, 23]), but special algorithms are needed for rigorous computation in order to control the wrapping effect (computed intervals growing too large to be useful), a known challenge with CAMP.

One way to control the wrapping effect is to use analytic interpolation, which we review next, followed by several other tools we use.

2.3 The compound matrix method

When computing the Evans function, one must carefully choose the numerical method for computing the Evans ODE. For example, suppose that $\{W_1^-(x), ..., W_k^-(x)\}$ is a basis for the solution space of the Evans ODE (3.3) that belongs to the unstable manifold of the fixed point zero at $x = -\infty$. The growth of these solutions near $x = -\infty$ is similar to that of

the solutions of the constant coefficient ODE, $Y'(x) = A_-Y(x)$. A basis for this solution space is given by terms of the form $e^{\nu x}v$ where ν is an eigenvalue of A_- with positive real part and v is an eigenvector corresponding to ν. When numerically solving for a basis $\{W_1^-(x), ..., W_k^-(x)\}$ of the unstable subspace at $x = -\infty$ of the ODE (3.3), any numerical error blows up in the direction corresponding to the eigenvalue of A_- with greatest real part. Further, components of the solution corresponding to smaller eigenvalues get lost at machine precision as the evolution of the ODE continues. Thus the computation is not numerically well-posed; see [10]. To overcome this, one may use the Compound Matrix Method.

The Compound Matrix Method is used to lift a manifold from $\mathbb{C}^n$ to the exterior product space $\wedge^k(\mathbb{C}^n)$. Note that $\wedge^k(\mathbb{C}^n) \cong \mathbb{C}^{\binom{n}{k}}$. If the dimension of the system is 20 and the dimension of the original manifold is 10, then the dimension of the lifted space is 184,756, which is not practical. However, for small dimensional systems, the lifted space is reasonable to work with and has the clear advantage that the k-dimensional manifold now corresponds to the one-dimensional manifold in the lifted system that corresponds to the largest growth rate.

Example: Let $n = 4$ and $k = 2$. Let $\{e_1, \ldots, e_4\}$ be the standard basis on $\mathbb{C}^4$. Our basis for $\wedge^2(\mathbb{C}^4)$ becomes $(e_1 \wedge e_2, e_1 \wedge e_3, e_1 \wedge e_4, e_2 \wedge e_4, e_3 \wedge e_4)$. Then we can lift a matrix B into $\wedge^2(\mathbb{C}^4)$ by defining $B^{(2)}$ as follows: $B^{(2)} \circ e_i \wedge e_j = (Be_i) \wedge e_j + e_i \wedge (Ae_j)$. Then if

$$B = \begin{pmatrix} b_{11} & b_{12} & b_{13} & b_{14} \\ b_{21} & b_{22} & b_{23} & b_{24} \\ b_{31} & b_{32} & b_{33} & b_{34} \\ b_{41} & b_{42} & b_{43} & b_{44} \end{pmatrix} \tag{2.9}$$

we get that

$$B^{(2)} = \begin{pmatrix} b_{11}+b_{22} & b_{23} & b_{24} & -b_{13} & -b_{14} & 0 \\ b_{32} & b_{11}+b_{33} & b_{34} & b_{12} & 0 & -b_{14} \\ b_{42} & b_{43} & b_{11}+b_{44} & 0 & b_{12} & b_{13} \\ -b_{31} & b_{21} & 0 & b_{22}+b_{33} & b_{34} & -b_{24} \\ -b_{41} & 0 & b_{21} & b_{43} & b_{22}+b_{44} & b_{23} \\ 0 & -b_{41} & b_{31} & -b_{42} & b_{32} & b_{33}+b_{44} \end{pmatrix}. \tag{2.10}$$

The resulting ODE that we wish to solve is given by

$$W' = B^{(k)}W, \quad W \in \mathbb{C}^{\binom{n}{k}}, \tag{2.11}$$

where μ_- is the sum of the eigenvalues of A_- with positive real part. This new ODE is numerically well-posed as now we are only evolving a one-dimensional manifold that corresponds to the largest growth mode. The Evans function is now the inner product of the one dimensional manifold coming from the left and from the right.

Now if we let $W = e^{\mu^- x}v(x)$, then $W' = \mu^- e^{\mu^- x}v(x) + e^{\mu^- x}v'(x)$. So $\mu^- e^{\mu^- x}v(x) + e^{\mu^- x}v'(x) = B^{(k)}e^{\mu^- x}v(x)$. Then our new ODE is:

$$\begin{cases} v'(x) & = (B^{(k)} - \mu^-)v(x) \\ v(-L) & = r^- \end{cases}$$

See [6] for details.

2.4 Analytic interpolation

Chebyshev polynomials are defined recursively as follows:

$$T_0(x) = 1, \quad T_1(x) = x, \quad T_n(x) = 2xT_{n-1}(x) + T_{n-2} \quad \text{for} \quad n > 2.$$

To interpolate with Chebyshev polynomials we represent a polynomial in the Chebyshev basis as $p_N(x) = \sum_{j=0}^{N-1} a_j T_j(x)$. To solve for the coefficients a_j, one may use the following

property,

$$\sum_{j=0}^{N-1} \cos(n\theta_j)\cos(m\theta_j) = \begin{cases} N & \text{if} \quad n = m = 0 \\ N/2 & \text{if} \quad n = m > 0 \\ 0 & \text{otherwise} \end{cases}$$

where $\theta_j = \frac{(j+\frac{1}{2})\pi}{N}$. Now note that if $f(x)$ is the function that we want to interpolate, we have the following:

$$f(x_j) = \sum_{n=0}^{N-1} a_n \cos(n\theta_j), \implies \sum_{n=0}^{N-1} a_n \sum_{j=0}^{N-1} \cos(m\theta_j)\cos(n\theta_j) = \sum_{j=0}^{N-1} \cos(m\theta_j) f(x_j),$$

$$\implies a_m = \frac{2 - \text{sgn }(m)}{N} \sum_{j=0}^{N-1} \cos(m\theta_j) f(x_j).$$

To determine the error associated with interpolating an analytic function f, we use the error bounds described in [32]. As detailed in these papers, if f is complex analytic inside and on the ellipse

$$E_\rho := \left\{ z \in \mathbb{C} | z = \frac{1}{2}\left(\rho e^{i\theta} + \frac{e^{-i\theta}}{\rho}\right) \theta \in [0, 2\pi] \right\},$$

then the error bound is given by

$$|f(x) - p_N(x)| \leq \frac{M_\rho L_\rho}{(\pi D_\rho \sinh \eta(N+1))},$$

where

$$\eta = \log \rho,\ D_\rho = \frac{1}{2}(\rho + \rho^{-1}) - 1,\ L_\rho = \pi\sqrt{\rho^2 + \rho^{-2}},\ M_\rho = \max_{z \in E_\rho}(|f(z)|).$$

2.5 Uniform Limit of Analytic Functions is Analytic

In obtaining a rigorous enclosure of the ODE solutions involved in computing the Evans function, we use series solutions of the ODE problem. These series solutions have analytic coefficients in the spectral parameter and these series converge as shown by bounding the truncation error with a geometric series. We need the theorem stated in this section to show the infinite series is analytic in the spectral parameter. We state the relevant definition and

theorem now.

Definition 7 (Locally Uniform Convergence)**.** Let $U \subset \mathbb{C}$ be an open set. Let $\langle f_n \rangle$ be a sequence of functions $f_n : U \to \mathbb{C}$. For $z \in U$, let $D_r(z)$ be the open disk of radius r about z. Then f_n converges to f locally uniformly if and only if for each $z \in U$, there is an $r \in \mathbb{R}_{>0}$ such that f_n converges uniformly to f on $D_r(z)$ and $D_r(z) \subset U$.

Theorem 8. *(Lang p156 [22]) [Uniform Limit of Analytic Functions is Analytic] Let U be an open subset of $\mathbb{C}$. Let $\langle f_n \rangle$ be a sequence of analytic functions, $f_n : U \to \mathbb{C}$. Let $\langle f_n \rangle$ converge locally uniformly to f on U. Then f is analytic.*

2.6 Bounds on Differential Equations

To interpolate the Evans function with analytic interpolation error bounds, we need to bound the ODE solutions associated with computing the Evans function. In doing so, the following theorem, which we quote from [9], is useful.

Theorem 9. *([9]) Consider the system of ordinary differential equations*

$$x' = f(t, x) \tag{2.12}$$

where x and f are n-dimensional vectors, and $0 \leq t < \infty$. We assume that $f(t, x)$ is continuous for $0 \leq t < \infty$, $|x| < \infty$, but we require no assumptions on f to assure the uniqueness of solutions of (2.12), as our arguments do not require uniqueness. Suppose that there exists a continuous non-negative function $\omega(t, r)$ on $0 \leq t < \infty$, $0 \leq r < \infty$, such that

$$|f(t, x)| \leq \omega(t, |x|), \;\; 0 \leq t < \infty, \;\; |x| < \infty. \tag{2.13}$$

It is well known [11, 40] that if $x(t)$ is a solution of (2.12), and $r(t)$ is the maximum solution of the scalar equation

$$r' = \omega(t, r) \tag{2.14}$$

with $r(0) = |x(0)|$, then $x(t)$ can be continued to the right as far as $r(t)$ exist, and

$$|x(t)| \leq r(t) \tag{2.15}$$

for all such t.

2.7 Parameterization Method for Vector Fields

In this section, we describe the parameterization method, which is key to our method of computer assisted proof. For details about this method, see [39].

Let us start with the stable manifold. Let $\eta \in \mathbb{R}^n$ be an equilibrium point for an analytic vector field $f : \mathbb{R}^n \to \mathbb{R}^n$. We also assume that $Df(\eta)$ has $m \leq n$ stable distinct eigenvalues $\lambda_1, \ldots, \lambda_m \in \mathbb{R}$. Then $Df(\eta)$ is diagonalizable, and we choose $\zeta_1, \ldots, \zeta_m \in \mathbb{R}$ to be the paired eigenvectors.

Our method is going to look at solutions of the following equation:

$$\lambda_1 \rho_1 \frac{\partial}{\partial \rho_1} \Psi(\rho_1, \ldots, \rho_m) + \ldots + \lambda_m \rho_m \frac{\partial}{\partial \rho_m} \Psi(\rho_1, \ldots, \rho_m) = f(\Psi(\rho_1, \ldots, \rho_m)). \tag{2.16}$$

If a function $\Psi : (-1, 1)^m \to \mathbb{R}^n$ solves (2.16) and fits the constraints:

$$\Psi(0, \ldots, 0) = \eta, \quad \text{and} \quad \frac{\partial}{\partial \rho_j} \Psi(0, \ldots, 0) = \eta_j, \quad 1 \leq j \leq m, \tag{2.17}$$

then it is a chart for some local stable manifold patch at η.

Note that if we rewrite 2.16 more simply, to better understand, we get:

$$D\Psi(\rho)\Lambda\rho = f(\Psi(\rho)). \tag{2.18}$$

Theorem 10. *(See [39].) Let ϕ represent the flow of f, and let Ψ be a solution of* (2.16) *that also satisfies* (2.17)*. Then Ψ is a one-to-one mapping and Ψ's image is a local stable manifold at η. Also,*

$$\phi(\Psi(\rho_1, \ldots, \rho_m), t) = \Psi(e^{\lambda_1 t}\rho_1, \ldots, e^{\lambda_m t}\rho_m),$$

for all $\rho = (\rho_1, \ldots, \rho_m) \in (-1, 1)^m$ and $t \geq 0$.

The proof of this theorem can be found in [39]. So Ψ tells us the embedding of the local stable manifold, and the dynamics on the manifold due to the conjugacy. We also know

that if η is hyperbolic, then the stable and unstable manifolds exist and are of the same smoothness as f.

2.8 Newton Kantorovich

To obtain a rigorous error bound on the numerical approximation of the solution to an ODE, we use the Newton-Kantorovich Theorem. This theorem allows us to get rigorous bounds on how good of an approximation one has to the zeros of a function. By setting up the ODE problem as a root finding problem, one can obtain bounds on the ODE solution approximation error via use of the Newton-Kantorovich theorem.

Theorem 11 (a-posteriori Newton-Kantorovich)**.** *(see [24])*

Suppose that $F : X \to Y$ is continuously differentiable and that $\bar{x} \in X, A^\dagger \in B(X,Y), A \in B(X,Y)$ with A one-to-one. Let $Y_0, Z_0, Z_1 > 0$ be positive constants, and $Z_2 : [0,\infty) \to [0,\infty)$ be a positive function, all satisfying the following conditions:

- $\|AF(\bar{x})\|_X \leq Y_0$
- $\|\mathbb{I} - AA^\dagger\|_{B(X)} \leq Z_0$
- $\|A(A^\dagger - DF(\bar{x})\|_{B(X)} \leq Z_1$
- $\sup_{x \in \overline{B_r(\bar{x})}} \|A(DF(\bar{x}) - DF(x))\|_{B(X)} \leq Z_2(r)r.$

If $p(r) := Z_2(r)r^2 - (1 - Z_0 - Z_1)r + Y_0$ is negative for some $r \in (0,\infty)$, then there is a unique $\tilde{z} \in B_r(\bar{z})$ such that $F(\tilde{z}) = 0$.

2.8.1 One-dimensional fixed point example. We demonstrate how to use the Newton-Kantorovich Theorem for rigorous computation by using it to prove that a fixed point exists for the function $g(x) = \sin x - 1$. We start by reformulating the problem as a root finding problem. We define $F(x) := \sin x - x - 1$. Thus, if $F(x_0) = 0$, we have $g(x_0) = x_0$. We use Newton's method to determine $\bar{x} := -1.934563211$ such that $F(\bar{x}) \approx 0$. We note that

Name of Bound	Bound
Y_0	$[0, 2.47975771 * 10^{-10}]$
Z_0	$[0, 5.33328937 * 10^{-12}]$
Z_1	$[0, 3.79422938 * 10^{-10}]$
$Z_2(r)$	$[0.6596664177, 0.7120642921]$

Table 2.1: Table of bounds needed for the Newton-Kantorovich Theorem.

$DF(x) = \cos x - 1$ and $D^2F(x) = -\sin x$. Now we let $A^\dagger = -1.355797141$, which comes from evaluating $\cos \bar{x} - 1$. Then $A = \frac{1}{A^\dagger} = -0.7375734686$. Now we will let $r_* = 0.1$ and $M = |\sin([\bar{x} - r_*, \bar{x} + r_*])|$, which gives us $M = [0.8943738431, 0.9654147315]$. Then we can finally find the bounds for the Newton-Kantorovich Theorem, which are given in Table 2.1

Then $p(r) = Z_2(r)r^2 - (1 - Z_0 - Z_1)r + Y_0 < 0$ for $r \in [-1.40437, -2.47976 * 10^{-10}]$. Thus $\sin x - 1$ has a unique fixed point x_* with $x_* \in [\bar{x} - 2.47976 * 10^{-10}, \bar{x} + 2.47976 * 10^{-10}]$.

2.8.2 2-Dimensional Root Example. We now demonstrate how to use the Newton-Kantorovich Theorem for a slightly more complicated rigorous computation. We prove a root exists for the following 2-d system:

$$f(x_1, x_2) = \begin{pmatrix} 2(x_1 - \pi) + \sinh x_2 \\ x_1 - 2x_2 - \pi \end{pmatrix}.$$

We will use the obvious root of $(\pi, 0)$ to inspire our guess at the zero,

$$\bar{x} = \begin{pmatrix} 3.141592654 \\ 0 \end{pmatrix}.$$

We will use a value of $r_* = 1 * 10^{-10}$. Now we need to calculate Df and evaluate it at our $\bar{x}$:

$$Df(x_1, x_2) = \begin{pmatrix} 2 & \cosh x_2 \\ 1 & -2 \end{pmatrix},$$

$$A^\dagger = Df(\bar{x}) = \begin{pmatrix} 2 & 1 \\ 1 & -2 \end{pmatrix}.$$

Next we calculate our $D^2 f(x_1, x_2)$ which ends up being $2 \times 2 \times 2$,

$$D^2_{x_1} f(x_1, x_2) = \begin{pmatrix} 0 & 0 \\ 0 & 0 \end{pmatrix},$$

$$D^2_{x_2} f(x_1, x_2) = \begin{pmatrix} 0 & \sinh x_2 \\ 0 & 0 \end{pmatrix}.$$

And then when we evaluate the derivatives at $\bar{x}$, yielding,

$$D^2_{x_1} f(\pi, 0) = \begin{pmatrix} 0 & 0 \\ 0 & 0 \end{pmatrix}, \quad D^2_{x_2} f(\pi, 0) = \begin{pmatrix} 0 & 0 \\ 0 & 0 \end{pmatrix}.$$

We choose

$$A^\dagger = \begin{pmatrix} 2 & 1 \\ 1 & -2 \end{pmatrix} \quad \text{and} \quad A = \begin{pmatrix} 0.4 & 0.2 \\ 0.2 & -0.4 \end{pmatrix}.$$

Then $\|A\|_M = 0.6$, which gives us:

$$f(\bar{x}) = 10^{-10} * \begin{pmatrix} 8.2041 \\ 4.1021 \end{pmatrix},$$

$$\|Af(\bar{x})\|_M = \left\| 10^{-10} * \begin{pmatrix} 4.1021 \\ 0 \end{pmatrix} \right\|_M \in [0, 4.1021 * 10^{-10}] = Y_0,$$

$$\|1 - AA^\dagger\| = 0 = Z_0,$$

$$\|A(A^\dagger - Df(\bar{x}))\| = 0 = Z_1,$$

$$M \in [0, 1 * 10^{-10}],$$

$$\|M * A\| \in [0, 4 * 10^{-10}] = Z_2.$$

Then plugging these values into the Newton-Kantorovich equation yields

$$p(r) = Z_2(r)r^2 - (1 - Z_0 - Z_1)r + Y_0 = (4 * 10^{-10})r^2 - r + 4.1021 * 10^{-10},$$

so that $p(r) < 0$ when $r = 10^{-9}$. Thus a root of f exists within a neighborhood of $\bar{x}$ of size 10^{-9}.

Chapter 3. A reaction-diffusion equation

We now demonstrate how we compute the Evans function rigorously to determine stability of a traveling wave solution. We illustrate our method with a scalar reaction-diffusion equation,

$$u_t = u_{xx} - u + u^2, \quad x \in \mathbb{R}. \tag{3.1}$$

A traveling wave solution satisfies the corresponding profile equation,

$$u'' = cu_x + u - u^2,$$

where $c \in \mathbb{R}$ is the wave speed. With zero wave-speed, a standing wave solution is given by $q(x) := (3/2)\,\mathrm{sech}^2(x/2)$.

We linearize (3.1) about the profile $q(x)$ and then seek separated solutions to obtain the eigenvalue problem

$$\lambda u = u'' + (2q - 1)u.$$

Writing this as a first order system, where $W = (w_1, w_2)^T = (u, u')^T$, we have

$$\begin{aligned} W'(x) &= A(x;\lambda)W(x), \\ A(x;\lambda) &:= \begin{pmatrix} 0 & 1 \\ 1 + \lambda - 2q(x) & 0 \end{pmatrix}. \end{aligned} \tag{3.2}$$

We define $A_\pm(\lambda) := \lim_{x\to\pm\infty} A(x;\lambda)$.

We note that the ODE given in (3.2) is invariant under the coordinate change $x \to -x$, $w_2 \to -w_2$. This invariance allows us to define the Evans function, without loss of generality,

as

$$D(\lambda) = w_1(0;\lambda)w_2(0;\lambda),$$

where $W : (-\infty, 0] \to \mathbb{R}^2$, $W(x;\lambda) = (w_1(x;\lambda), w_2(x;\lambda))^T$, is a solution of (3.2) that belongs to the unstable manifold of the fixed point zero.

As detailed in Section 2.2, the Evans function is constructed by solving for a basis of solutions of (3.2) that belong to the unstable manifold at $x = -\infty$, and for a basis of solutions of (3.2) that belong to the stable manifold at $x = +\infty$, and then forming a matrix for these solutions and evaluating the determinant of that matrix at $x = 0$. For this simple example, the unstable and stable manifolds are one dimensional. In this situation, to make (3.2) better conditioned, it is standard practice to factor out the asymptotic growth of the ODE solution as $x \to \pm\infty$. This rescaling is accomplished by defining a function V by $W(x) = e^{\mu x}V(x)$, where μ is the the eigenvalue of A_- with positive real part, or the eigenvalue of A_+ with negative real part. The new ODE to solve is then of the form $V'(x) = (A(x;\lambda) - \mu I)V(x)$. The solution V posed on a half-line converges at asymptotic rate as $x \to \pm\infty$ to the eigenvector of $A_\pm$ that corresponds to μ. We recall that under the rescaling, $W(0) = V(0)$, so the roots of the Evans function remain the same.

In our computer assisted proof, we make a different choice than the usual one for rescaling (3.2), which allows us to use the parameterization method, described in Section 2.7, to obtain a tight enclosure of the solution to (3.2) on an interval $(-\infty, x_0]$ for some $x_0 < 0$. In particular, we rescale (3.2) via $W(x) = e^{\mu x}V(x)$ where μ is chosen so that the positive eigenvalue of $A_- - \mu I$ is the same as that of the Jacobian of the profile ODE. If we do not make this scaling choice for μ, the series expansion for the solution to (3.2) will have a different basis than the series expansion for the solution of the profile equation. If we use the usual scaling used in an Evans function computation, then the solution we seek will belong to the center manifold rather than the unstable manifold, and there will not be an analytic expansion of the solution in the basis we use. Thus, our careful choice of the scaling factor μ is key to the method.

For the scalar reaction-diffusion system (3.1), choosing $\mu = \sqrt{1+\lambda} - 1$ results in $A_- - \mu I$ having a single positive eigenvalue, $1 \in \sigma(A_- - \mu I)$, which corresponds to the single positive eigenvalue of the Jacobian of the profile ODE equation evaluated at the fixed point zero. Parameterizing by μ, rather than by the spectral parameter λ, leads to the new ODE system to solve,

$$\begin{aligned} V'(x) &= (A(x;\mu)W(x), \\ A(x;\mu) &:= \begin{pmatrix} -\mu & 1 \\ (\mu+1)^2 - 2q(x) & -\mu \end{pmatrix}. \end{aligned} \tag{3.3}$$

We newly define $A_\pm(\mu) := \lim_{x\to\pm\infty} A(x;\mu)$.

To obtain a rigorous enclosure of a solution of (3.3) on the interval $(-\infty, 0]$ belonging to the unstable manifold of the fixed point zero, we carry out the following steps:

(i) We augment (3.3) with the profile equation to form a larger system.

(ii) We formulate finding the solution of this augmented system as a root finding problem.

(iii) We obtain a solution of the augmented system on the interval $(-\infty, x_0]$ for some $x_0 < 0$ using the parameterization method.

(iv) We obtain a solution of the augmented system on small intervals $[x_j, x_{j+1}]$, where $x_0 < x_1 < x_2 < ... < x_J$, via a series solution.

(v) We use the Newton-Kantorovich Theorem, described in Section 2.8, to obtain a rigorous bound on the error of our numerical approximation of the solution to the augmented problem.

The augmented system is given by

$$\begin{pmatrix} y \\ z \\ v \\ w \end{pmatrix}' = \begin{pmatrix} z \\ y - y^2 \\ w - \mu v \\ ((\mu+1)^2 - 2y)v - \mu w \end{pmatrix}, \tag{3.4}$$

where $\mu = \sqrt{1+\lambda} - 1$, the first two components are the profile equation, and the last two components are those given in (3.3).

3.1 Formulating a zero finding problem

Next, we form a function whose roots correspond to the existence of an ODE solution of (3.4). First, we define $\Phi(\theta)$ to be a parameterization of the unstable manifold of the fixed point zero of the ODE system (3.4). We define $\Phi(y, z, v, w, \Delta x)$ to be the solution at Δx of the initial value problem (3.4) with initial conditions (y, z, v, w) at $x = 0$. We then form the function

$$F(X) = \begin{pmatrix} V_0 - \Phi(\theta) \\ V_1 - \psi_0(V_0, \Delta x) \\ V_2 - \psi_1(V_1, \Delta x) \\ \vdots \\ V_N - \psi_{N-1}(V_{N-1}, \Delta x) \\ z_N \end{pmatrix}$$

where $X = (\theta, y_0, z_0, v_0, w_0, y_1, z_1, v_1, w_1, \cdots, y_N, z_N, v_N, w_N)$ and

$$V_k = \begin{pmatrix} y_k & z_k & v_k & w_k \end{pmatrix}^T.$$

The zero of F will give the solution to (3.3) at the nodes

$$x_0 = -N\Delta x < x_1 < ... < x_N = 0,$$

where $x_{j+1} - x_j = \Delta x$ for each $0 \leq j \leq N-1$. That is, (y_j, z_j, v_j, w_j) is the value of the solution to (3.3) at x_j. This is demonstrated in Figure 3.1. Red dots indicate the ordered

pairs (x_j, y_j). The solid black line indicates the actual profile solution.

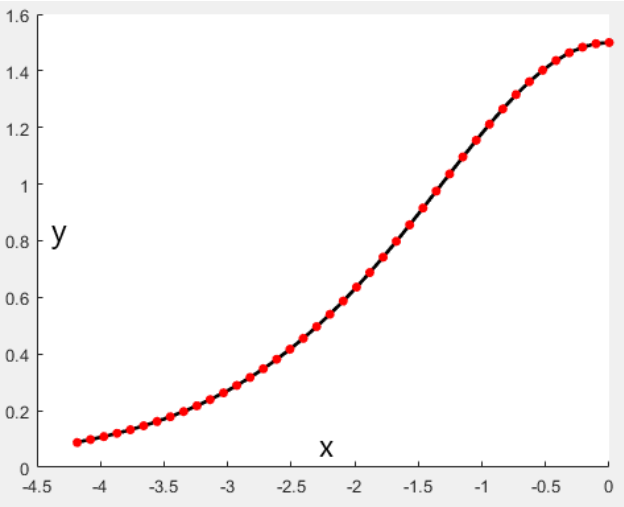

Figure 3.1: Plot of the profile solution with a solid line, and plots of the ordered pairs (x_j, y_j) that form some of the components of the vector that is a root of F.

To apply the Newton-Kantorovich Theorem to obtain a rigorous bound on the error of a good approximation $\bar{X}$ of the zero of F, we need the Jacobian of F, which is given by

$$DF(X) = \begin{pmatrix} -\frac{d\Phi}{d\theta} & I_{4\times 4} & 0 & \cdots & 0 & 0 \\ 0 & -D\psi(V_0, \Delta x) & I_{4\times 4} & \cdots & 0 & 0 \\ 0 & 0 & -D\psi(V_1, \Delta x) & I_{4\times 4} & \cdots & 0 \\ \vdots & \vdots & \vdots & \ddots & \vdots & \vdots \\ 0 & 0 & 0 & \cdots & -D\psi(V_{N-1}, \Delta x) & I_{4\times 4} \\ 0 & 0 & 0 & \ddots & 0 & e_2^T \end{pmatrix},$$

where e_2^T is the standard Euclidean basis vector $(0, 1, 0, 0)^T$.

We also need the second derivative D_2F, which we do not record here as it is a large 3D array, but we note that it is convenient to code it by using a for loop ranging from 1 to N and using the fact that DF is band-diagonal.

Next, we describe how we obtain a rigorous enclosure of the parameterization $\Phi(\theta)$ of the unstable manifold of the fixed point zero of (3.3).

3.2 Parameterization of the unstable manifold

We obtain a solution of (3.3) on the interval $(-\infty, x_0]$ that belongs to the unstable manifold of the fixed point zero by making the Ansatz that

$$\begin{pmatrix} y(x) \\ z(x) \\ v(x) \\ w(x) \end{pmatrix} = \sum_{n=0}^{\infty} \begin{pmatrix} y_n \\ z_n \\ v_n \\ w_n \end{pmatrix} \theta^n(x),$$

where $\theta(x) = \theta_0 e^x$ and $\theta_0 \in \mathbb{R}$ is constant. Plugging the Ansatz into (3.3), we obtain

$$\begin{pmatrix} \sum_{n=0}^{\infty} y_n \theta^n(x) \\ \sum_{n=0}^{\infty} z_n \theta^n(x) \\ \sum_{n=0}^{\infty} v_n \theta^n(x) \\ \sum_{n=0}^{\infty} w_n \theta^n(x) \end{pmatrix}' = \begin{pmatrix} \sum_{n=0}^{\infty} z_n \theta^n(x) \\ \sum_{n=0}^{\infty} y_n \theta^n(x) - \left(\sum_{n=0}^{\infty} y_n \theta^n(x)\right)^2 \\ \sum_{n=0}^{\infty} w_n \theta^n(x) - \mu \sum_{n=0}^{\infty} v_n \theta^n(x) \\ -2\left(\sum_{n=0}^{\infty} y_n \theta^n(x)\right)\left(\sum_{n=0}^{\infty} v_n \theta^n(x)\right) + (1+\lambda) \sum_{n=0}^{\infty} v_n \theta^n(x) - \mu \sum_{n=0}^{\infty} w_n \theta^n(x) \end{pmatrix}.$$

This leads to the following recurrence relation for $n \geq 2$,

$$\left[nI - \begin{pmatrix} 0 & 1 & 0 & 0 \\ 1 & 0 & 0 & 0 \\ 0 & 0 & -\mu & 1 \\ 0 & 0 & (\mu+1)^2 & -\mu \end{pmatrix} \right] \begin{bmatrix} y_n \\ z_n \\ v_n \\ w_n \end{bmatrix} = \begin{pmatrix} 0 \\ -\sum_{k=1}^{n-1} y_{n-k} y_k \\ 0 \\ -2 \sum_{k=1}^{n-1} y_{n-k} v_k \end{pmatrix}. \tag{3.5}$$

We define

$$B_n := \begin{pmatrix} n & -1 & 0 & 0 \\ -1 & n & 0 & 0 \\ 0 & 0 & n+\mu & -1 \\ 0 & 0 & -(\mu+1)^2 & n+\mu \end{pmatrix},$$

and note that B_n is invertible with inverse

$$B_n^{-1} = \begin{pmatrix} \frac{n}{n^2-1} & \frac{1}{n^2-1} & 0 & 0 \\ \frac{1}{n^2-1} & \frac{n}{n^2-1} & 0 & 0 \\ 0 & 0 & \frac{n+\mu}{(n+\mu)^2-(\mu+1)^2} & \frac{1}{(n+\mu)^2-(\mu+1)^2} \\ 0 & 0 & \frac{(\mu+1)^2}{(n+\mu)^2-(\mu+1)^2} & \frac{n+\mu}{(n+\mu)^2-(\mu+1)^2} \end{pmatrix},$$

so long as $(n+\mu)^2-(\mu+1)^2 \neq 0$. For $\Re(\lambda) \geq 0$, we have $\Re(\mu) \geq 0$, and so B_n is always invertible for $n \in \mathbb{N}$, $n \geq 2$. That is, there are no resonances. Thus we can solve for $(y_n, z_n, v_n, w_n)^T$ in equation (3.5).

The series is initialized with $(y_0, z_0, v_0, w_0) = (0,0,0,0)$ and with the first order coefficients given by $(y_1, z_1, v_1, w_1) = (1,1,1,1+\mu)$, the eigenvector with corresponding eigenvalue 1 of the Jacobian of (3.4) evaluated at the fixed point zero,

$$J(0,0,0,0) = \begin{pmatrix} 0 & 1 & 0 & 0 \\ 1 & 0 & 0 & 0 \\ 0 & 0 & -\mu & 1 \\ 0 & 0 & (\mu+1)^2 & -\mu \end{pmatrix}.$$

With these choices and inside the radius of convergence of the series, the series gives a solution of (3.4) that belongs to the unstable manifold of the fixed point zero. The parameterization of the unstable manifold of interest is thus given by

$$\Phi(\theta) = \sum_{n=0}^{\infty} (y_n, z_n, v_n, w_n)^T \theta^n.$$

To determine a lower bound on the radius of convergence of the series, we bound the series by a geometric series as described in the following proposition.

Proposition 12. *If* $\Re(\mu) \geq -1$ *and* $C = 4 \cdot \max(1, |1+\mu|)$, *then*

$$|y_n|, |z_n|, |v_n|, |w_n| \leq \left(\frac{1}{2}\right)^{n+1} C^n$$

for all $n \in \mathbb{N} \cup \{0\}$.

Proof. We first recall that $y_0 = z_0 = v_0 = w_0 = 0$, so the result is true for $n = 0$. We recall that $(y_1, z_1, v_1, w_1) = (1,1,1,1+\mu)$, so the result is true for $n = 1$. Let $n \geq 2$ be an integer. Assume that the result holds for indices 0 through $n-1$. We show that $|w_n| \leq \left(\frac{1}{2}\right)^{n+1} C^n$. Showing the other three nth coefficients satisfy this bound is similar, but more straight

foward. Using B_n^{-1} to solve (3.5), we have

$$\begin{aligned}
|w_n| &\leq \left| -2\frac{n+\mu}{(n-1)(n+1+2\mu)} \sum_{k=1}^{n-1} y_{n-k} v_k \right| \\
&\leq 2\frac{n+\mu}{(n-1)(n+1+2\mu)} \sum_{k=1}^{n-1} \left(\frac{1}{2}\right)^{n+2} C^n \\
&\leq \left(\frac{1}{2}\right)^{n+1} C^n \left[\frac{n+\mu}{n+\mu+(1+\mu)}\right] \\
&\leq \left(\frac{1}{2}\right)^{n+1} C^n.
\end{aligned}$$

□

When using the Newton-Kantorovich Theorem, we need to compute $\Phi(\theta)$ and its first two derivatives. Let $r = |C\theta/2|$ where $C = 4 \cdot \max(1, |1+\mu|)$. If $r \geq 1$, the geometric series bounding the coefficients of Φ does not converge. Otherwise, excluding the terms of the series of index $N+1$ or bigger, the truncation error bound satisfies

$$\begin{aligned}
\left| \sum_{n=N+1}^{\infty} \chi_n \theta^n \right| &\leq \frac{1}{2} \sum_{n=N+1}^{\infty} r^n, \\
&\leq \frac{1}{2} \frac{r^{N+1}}{1-r},
\end{aligned}$$

where χ_n represents y_n, z_n, v_n, or w_n. To bound the truncation error involved in computing $\Phi'(\theta)$ and $\Phi''(\theta)$, we define $f(r) := \frac{1}{2}\frac{r^{N+1}}{1-r}$. The bound on the truncation error involved in computing $\Phi'(\theta)$ is $\frac{Cf'(r)}{4}$, and for $\Phi''(\theta)$ it is $\frac{C^2 f''(r)}{8}$.

Next, we obtain the recurrence relation for the series solution over a finite interval.

3.3 Series solution on a finite interval

To obtain the solution of (3.4) as an initial value problem with initial condition $(y_0, z_0, v_0, w_0)^T$ at $x = 0$, we make the ansatz

$$(y(\Delta x), z(\Delta x), v(\Delta x), w(\Delta x)) = \sum_{n=0}^{\infty} (y_n, z_n, v_n, w_n)(\Delta x)^n.$$

The recurrence relations are thus given by

$$\begin{aligned}
y_{n+1} &= \frac{z_n}{n+1}, \\
z_{n+1} &= \frac{1}{n+1}\left(y_n - \sum_{k=0}^{n} y_k y_{n-k}\right), \\
v_{n+1} &= \frac{1}{n+1}\left(w_n - \mu v_n\right), \\
w_{n+1} &= \frac{1}{n+1}\left((\mu+1)^2 v_n - \mu w_n - 2\sum_{k=0}^{n} y_k v_{n-k}\right),
\end{aligned}$$

for $n \geq 1$, where y_0, z_0, v_0, w_0 are given by the initial condition.

We define $\chi = (y_0,\ z_0,\ v_0, w_0)^T$. For $1 \leq i \leq 4$, we obtain the derivatives

$$\begin{aligned}
\frac{\partial y_{n+1}}{\partial \chi_i} &= \frac{1}{n+1}\frac{\partial z_n}{\partial \chi_i}, \\
\frac{\partial z_{n+1}}{\partial \chi_i} &= \frac{1}{n+1}\left(\frac{\partial y_n}{\partial \chi_i} - \sum_{k=0}^{n}\left(\frac{\partial y_k}{\partial \chi_i} y_{n-k} + y_k \frac{\partial y_{n-k}}{\partial \chi_i}\right)\right), \\
\frac{\partial v_{n+1}}{\partial \chi_i} &= \frac{1}{n+1}\left(\frac{\partial w_n}{\partial \chi_i} - \mu\frac{\partial v_n}{\partial \chi_i}\right), \\
\frac{\partial w_{n+1}}{\partial \chi_i} &= \frac{1}{n+1}\left((\mu+1)^2\frac{\partial v_n}{\partial \chi_i} - \mu\frac{\partial w_n}{\partial \chi_i} - 2\sum_{k=0}^{n}\left(\frac{\partial y_k}{\partial \chi_i} v_{n-k} + y_k \frac{\partial v_{n-k}}{\partial \chi_i}\right)\right).
\end{aligned}$$

We note that

$$\frac{\partial y_{n+1}}{\partial v_0} = \frac{\partial y_{n+1}}{\partial w_0} = \frac{\partial z_{n+1}}{\partial v_0} = \frac{\partial z_{n+1}}{\partial w_0} = 0.$$

The second derivatives are then given by

$$\begin{aligned}
\frac{\partial^2 y_{n+1}}{\partial \chi_i \partial \chi_j} &= \frac{1}{n+1}\frac{\partial^2 z_n}{\partial \chi_i \partial \chi_j}, \\
\frac{\partial^2 z_{n+1}}{\partial \chi_i \partial \chi_j} &= \frac{1}{n+1}\left(\frac{\partial^2 y_n}{\partial \chi_i \partial \chi_j} - \sum_{k=0}^{n}\left(\frac{\partial^2 y_k}{\partial \chi_i \partial \chi_j} y_{n-k} + \frac{\partial y_k}{\partial \chi_i}\frac{\partial y_{n-k}}{\partial \chi_j} + \frac{\partial y_k}{\partial \chi_j}\frac{\partial y_{n-k}}{\partial \chi_i} + y_k \frac{\partial^2 y_{n-k}}{\partial \chi_i \partial \chi_j}\right)\right), \\
\frac{\partial^2 v_{n+1}}{\partial \chi_i \partial \chi_j} &= \frac{1}{n+1}\left(\frac{\partial^2 w_n}{\partial \chi_i \partial \chi_j} - \mu\frac{\partial^2 v_n}{\partial \chi_i \partial \chi_j}\right), \\
\frac{\partial^2 w_{n+1}}{\partial \chi_i \partial \chi_j} &= \frac{1}{n+1}\left((\mu+1)^2\frac{\partial^2 v_n}{\partial \chi_i \partial \chi_j} - \mu\frac{\partial^2 w_n}{\partial \chi_i \partial \chi_j}\right) \\
&\quad - \frac{2}{n+1}\sum_{k=0}^{n}\left(\frac{\partial^2 y_k}{\partial \chi_i \partial \chi_j} v_{n-k} + \frac{\partial y_k}{\partial \chi_i}\frac{\partial v_{n-k}}{\partial \chi_j} + \frac{\partial y_k}{\partial \chi_i}\frac{\partial v_{n-k}}{\partial \chi_j} + y_k \frac{\partial^2 v_{n-k}}{\partial \chi_i \partial \chi_j}\right).
\end{aligned}$$

Next, we establish a result which allows us to use computer assisted proof to bound the

coefficients and their first two derivatives by a geometric series.

Proposition 13. *Let $N \in \mathbb{N}$, $m \in \mathbb{N}$, $C > 0$, and define $C_0 = 2^m \max(|y_0|, |z_0|, |v_0|, |w_0|)$. If for all $0 \leq n \leq N$ and each $\phi_n \in \{y_n, z_n, v_n, z_n\}$ it holds that $|\phi_n|,\ |\frac{\partial \phi_n}{\partial \chi_i}|,\ |\frac{\partial^2 \phi_n}{\partial \chi_i \partial \chi_j}| \leq \frac{C_0 C^n}{2^m}$, and if*

$$\begin{aligned} 1 \geq & \frac{1}{C}\left(\frac{1}{N+1} + 2^{2-m} C_0\right), \\ 1 \geq & \frac{1+|\mu|}{C(N+1)}, \\ 1 \geq & \frac{|1+\mu|^2 + |\mu|}{C(N+1)} + \frac{2^{3-m} C_0}{C}, \end{aligned}$$

then $|y_n|,\ |z_n|,\ |v_n|,\ |w_n| \leq \frac{C_0 C^n}{2^m}$ for all integers $n \geq 0$.

Proof. We prove the result for $\frac{\partial^2 w_{n+1}}{\partial \chi_i \partial \chi_j}$ using induction. Proving the result for the other terms is similar, but less involved. Assume the hypothesis holds. Let $n \geq N$ be an integer. We note the following bounds on representative terms, which hold by the inductive hypothesis,

$$\begin{aligned} \left|\frac{\partial^2 y_n}{\partial \chi_i \partial \chi_j}\right| &\leq \frac{C_0 C^n}{2^m} \\ \left|\frac{\partial y_k}{\partial \chi_i}\frac{\partial v_{n-k}}{\partial \chi_j}\right| &\leq \frac{C_0^2 C^n}{2^{2m}}, \\ \left|\frac{\partial^2 y_k}{\partial \chi_i \partial \chi_j} v_{n-k}\right| &\leq \frac{C_0^2 C^n}{2^{2m}}. \end{aligned}$$

Using the appropriate analogous bounds on all the terms, we see that

$$\begin{aligned} \left|\frac{\partial^2 w_{n+1}}{\partial \chi_i \partial \chi_j}\right| &\leq \frac{1}{n+1}\left((|\mu+1|^2 + |\mu|) C_0 C^n 2^{-m} + 2\sum_{k=0}^{n} 4\frac{C_0 C^n}{2^m}\right), \\ &\leq C_0 C^{n+1} 2^{-m}\left(\frac{|\mu+1|^2 + |\mu|}{C(n+1)} + \frac{2^{3-m} C_0}{C}\right). \end{aligned}$$

Hence, if $1 \geq \frac{|1+\mu|^2+|\mu|}{C(N+1)} + \frac{2^{3-m}C_0}{C}$, then $\left|\frac{\partial^2 w_{n+1}}{\partial \chi_i \partial \chi_j}\right| \leq C_0 C^{n+1} 2^{-m}$. Thus, by induction the result holds for all integers $n \geq 0$. □

With these propositions in place, we are ready to use the Newton-Kantorovich Theorem described in Section 2.8.

3.4 Newton Kantorovich Theorem

Applying the Newton Kantorovich Theorem described in Section 2.8 to the function F described in Section 3.1, we obtain a rigorous enclosure of the Evans function for a single value of μ. We record statistics for the case that $\mu = 1$.

We choose θ_L so that x_0 corresponds to $x = -5$. We use $\Delta x = 0.1$. We obtain an initial guess $\bar{x}$ to the zero of F by computing with double arithmetic the solution to (3.4) initialized with $\Phi(\theta_L)$. We use the first 21 terms of the series to compute $\Phi(\theta)$, and we use the first 36 terms of the series to rigorously approximate the solution of (3.4) over an interval of width Δx, although we only use 21 terms to compute the second derivative as only a rough upper bound on the modulus is needed. We took $r = 5e-9$ to compute $p(r)$ in the Newton-Kantorovich Theorem, though we bounded the second derivative using $r = 1e-5$.

We choose $A^\dagger$ to be the midpoint of the Jacobian, DF, of F. We use double arithmetic to set A to the numerical approximation of the inverse of $A^\dagger$.

The resulting bounds associated with the Newton-Kantorovich Theorem are

$$\begin{aligned} Y_0 &\approx 6.850 \times 10^{-10} \\ Z_0 &\approx 8.559 \times 10^{-13} \\ Z_1 &\approx 2.7710 \times 10^{-10} \\ Z_2(r) &\approx 7.2521 \times 10^{5} \\ p(r) &= Z_2(r)4^2 - (1 - Z_0 - Z_1)r + Y_0|_{r=5e-9} \\ &\approx -4.296 \times 10^{-9}. \end{aligned}$$

Since $p(5e-9) < 0$, the zero of F lies within $r = 5e-9$ of the initial guess $\bar{x}$. It took 833 seconds to run the code.

The next step is to determine for which values of μ we need to compute the Evans function. In the next section, we obtain a bound on the modulus of unstable eigenvalues, which in turn gives a bound on μ.

3.5 Energy Estimate

We recall that the reaction-diffusion equation of interest is given by

$$u_t = u_{xx} - u + u^2. \tag{3.6}$$

Recall that a standing wave solution is given by $q(x) := (3/2)\,\mathrm{sech}^2(x/2)$. Linearizing (3.6) about the standing wave q, and looking for separated solutions leads to the eigenvalue problem

$$\lambda u = u'' - u + 2qu. \tag{3.7}$$

We note that the essential spectrum consists of $(-\infty, -1]$. We use an energy estimate to obtain a bound on how large the modulus of an unstable eigenvalue can be. We multiply both sides of (3.7) by $\bar{u}$ and integrate over the real line to obtain

$$\begin{aligned} \lambda \|u\|_{L^2}^2 &= -\|u\|_{L^2}^2 + \int_{-\infty}^{\infty} \bar{u}u'' + 2\int_{-\infty}^{\infty} qu\bar{u} \\ &= -\|u\|_{L^2}^2 - \|u'\|_{L^2}^2 + 2\int_{-\infty}^{\infty} q|u|^2, \end{aligned} \tag{3.8}$$

where the last line comes from doing integration by parts on the second term. Taking the real part of (3.8) leads to

$$\begin{aligned} \Re(\lambda)\|u\|_{L^2}^2 &\leq 2\|q\|_\infty \|u\|_{L^2}^2 - \|u\|_{L^2}^2 - \|u'\|_{L^2}^2 \\ &\leq 2\|u\|_{L^2}^2, \end{aligned}$$

since $\|q\|_\infty \leq 3/2$. Thus, $\Re(\lambda) \leq 2$. Since the right hand side of (3.8) is real valued, we conclude $\Im(\lambda) = 0$. Thus it suffices to find any point spectra in the real interval $[0, 2]$.

The next step is to determine where nodes should be placed in the interval $[0, 2]$ for analytic interpolation.

3.6 Analytic interpolation

We now describe the various choices we make to carry out analytic interpolation, as described in Section 2.4. We use the coordinate change $\mu = (\mu_L + \mu_R)/2 + (\mu_R - \mu_L)\tilde{\mu}/2$, where

$\tilde{\mu} \in [-1, 1]$ and μ_L and μ_R are the left and right bounds of the values of μ that we consider. We choose $\rho = 3$ and verify that $\Re(\mu) > -0.5$ for $\tilde{\mu}$ inside and on the ellipse given by $E_\rho := \{(\rho e^{i\theta} + \rho^{-1} e^{-i\theta})/2\}$. We then divide $[0, 2\pi]$ into 10 equally spaced intervals and obtain a bound, using interval arithmetic computations, on the modulus of the Evans function evaluated at each of those subintervals. To bound the Evans function, we evaluate $\Phi(\theta_L)$ and verify that the series, by which $\Phi(\theta_L)$ is defined, converges. This gives a bound on the size of the solution $(y, z, v, w)^T$ of (3.4) at x_0. We then use the method described in Section 2.6 to obtain a crude bound on the growth of the solutions over the interval $[x_0, 0]$. We then use these bounds to bound the modulus of $D(\mu) = v(0)w(0)$. We request that the interpolation error be no more than 10^{-10}, which results in the number of interpolation nodes needed being 59.

3.7 Results

In Figure 3.2 we plot the Evans function, as computed rigorously, against the spectral parameter λ at the interpolated nodes needed for rigorous interpolation. We note that the sign of the Evans function changes at approximately $\lambda = 1.25$, which indicates the existence of an unstable eigenvalue.

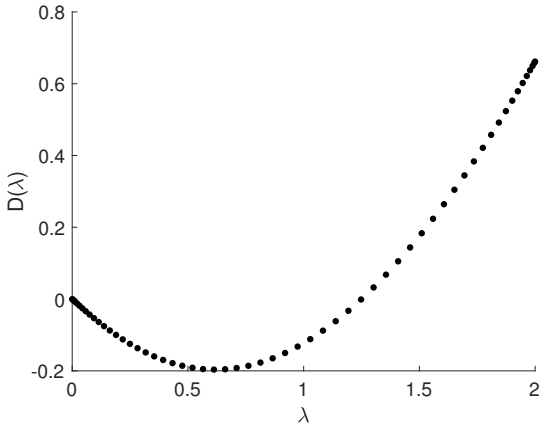

Figure 3.2: Plot of the rigorously computed Evans function at the nodes needed for rigorous interpolation.

If the there were no eigenvalues and we wanted to prove the wave is stable, we would choose enough interpolation nodes to have a good approximation of the derivative of the Evans function by the derivative of the Chebyshev interpolant; see [32, 37]. We would then evaluate the interpolant all along the interval $[0, 2]$ to ensure that there are no zeros of the Evans function except at $\lambda = 0$. In a small neighborhood of $\lambda = 0$, the interval enclosure of the Evans function evaluation would include zero. However, in that neighborhood, we would use the derivative of the interpolant to show that the derivative is of one sign only, hence the Evans function has only one zero at the origin.

With this scalar reaction-diffusion model, we have demonstrated how to obtain rigorous error bounds on the computation of the Evans function. We recall a few key points of this method before demonstrating in the next chapter how to deal with some other situations that arise when computing the Evans function for other systems.

(i) Using the parameterization method is essential in order to represent the solution of (3.4) on the interval $(-\infty, x_0]$. We note that the choice of θ_L for all values of the spectral parameter λ makes it so $\Phi(\theta_L; \mu)$, which is $\Phi(\theta_L)$ for a given μ, varies analytically with respect to μ. This is important in order for the Evans function to be analytic.

(ii) The careful choice of scaling factor μ is key to be able to represent the unstable manifold of the fixed point zero of (3.4) using the parameterization method. We must choose μ so that an analytic solution exists for the manifold we wish to obtain.

(iii) The use of the standard polynomial basis for the series solution on the finite intervals of width Δx is convenient since we can use a proof by induction to bound the coefficients of the series with a geometric series. We note that many other rigorous methods work for computing the solution on these intervals, including the use of a series with a basis consisting of the Chebyshev polynomials. Some of these other methods are far more computationally efficient, but also more involved to implement.

(iv) Finally, we note that in more complicated systems, one may have to solve for an unstable or stable manifold that is of dimension larger than one. We outline how to deal with this situation in the next chapter.

Chapter 4. Multi-dimensional manifolds

In this chapter, we use the Gray-Scott system to demonstrate how to deal with the situation that the dimension of the stable/unstable manifold of a fixed point (the limit of the profile as $x \to \pm\infty$) of the profile equation is greater than one. All other aspects of rigorously computing the Evans function are demonstrated in Chapter 3. We begin by introducing the system.

4.1 The Gray-Scott system

The Gray-Scott system of equations is given by

$$\begin{aligned} u_t &= u_{xx} - uv^2 + \alpha(1-u), \\ v_t &= v_{xx} + uv^2/\gamma - v/\gamma, \end{aligned} \tag{4.1}$$

where $\alpha, \gamma > 0$. A stationary traveling wave solution satisfies the profile equations,

$$\begin{aligned} u'' &= uv^2 - \alpha(1-u), \\ v'' &= \frac{1}{\gamma}(v - uv^2). \end{aligned} \tag{4.2}$$

Setting $w = u'$, and $z = v'$, we arrive at the first order system,

$$\begin{pmatrix} u \\ w \\ v \\ z \end{pmatrix}' = \begin{pmatrix} w \\ uv^2 - \alpha(1-u) \\ z \\ \frac{1}{\gamma}(v - uv^2) \end{pmatrix}. \tag{4.3}$$

The Jacobian of this system is given by,

$$J = \begin{pmatrix} 0 & 1 & 0 & 0 \\ v^2 + \alpha & 0 & 2uv & 0 \\ 0 & 0 & 0 & 1 \\ \frac{-v^2}{\gamma} & 0 & \frac{1}{\gamma}(1 - 2uv) & 0 \end{pmatrix}. \tag{4.4}$$

The fixed points of the system (4.1) are $(1, 0, 0, 0)^T$ and $(u_0, 0, 1/u_0, 0)^T$, where we define $u_0 := \frac{1 \pm \sqrt{1 - 4/\alpha}}{2}$. The eigenvalues of the Jacobian evaluated at the fixed point $(1, 0, 0, 0)^T$ are given by $\mu_1^{\pm} = \pm\sqrt{\alpha}$ and $\mu_2^{\pm} = \pm\frac{1}{\sqrt{\gamma}}$. Corresponding eigenvectors are given by $(1, \mu_1^{\pm}, 0, 0)^T$ and $(0, 0, 1, \mu_2^{\pm})^T$, respectively.

We note that the unstable manifold of the fixed point that corresponds to $x = -\infty$ is two-dimensional, as is the stable manifold of the fixed point that corresponds to $x = +\infty$. Parameterizing these manifolds is more involved then what we described in Chapter 3 since the manifolds are now two-dimensional. To parameterize the unstable manifold of the fixed point $(1, 0, 0, 0)$, we make the ansatz

$$\begin{pmatrix} u(x) \\ v(x) \end{pmatrix} = \sum_{m,n=0}^{\infty} \begin{pmatrix} u_{mn} \\ v_{mn} \end{pmatrix} \left(\theta_1^0 e^{\mu_1^+ x}\right)^m \left(\theta_2^0 e^{\mu_2^+ x}\right)^n.$$

The unstable manifold is then parameterized by $\theta_1 := \theta_1^0 e^{\mu_1^+ x}$ and $\theta_2 := \theta_2^0 e^{\mu_2^+ x}$. This again leads to a recursion formula that we can show yields coefficients that are bounded by a geometric series inside a certain radius. The main difference is in how we rescale the Evans function given that the profile requires an ansatz of this form. We recall that for the system described in Chapter 3, we rescaled the Evans function which in practice resulted in subtracting μ multiplied by the identify from the matrix $A(x; \lambda)$ given in (3.3). We recall that μ was chosen so that the eigenvector corresponding to the eigenvalue of A_- with positive real part was an eigenvector of the rescaled system, $A_- - \mu I$, with corresponding eigenvalue matching that of the Jacobian of the profile ODE. The main point of this chapter is to describe how to rescale the Evans function (what to choose for μ) when the parameterization of the profile in a neighborhood of infinity is multidimensional.

Before discussing this issue, we must introduce some additional details, but we first note that when $\alpha\gamma = 1$ and $0 < \gamma < \frac{2}{9}$, an analytic solution (see [17]) is given by

$$\begin{aligned} u(t) &= 1 - \frac{3\gamma}{1 + Q\cosh(t/\sqrt{\gamma})}, \\ v(t) &= \frac{3}{1 + Q\cosh(t/\sqrt{\gamma})}, \end{aligned} \tag{4.5}$$

where $Q := \sqrt{1 - 9\gamma/2}$. Derivatives of the profile are given by

$$\begin{aligned} u'(t) &= -\frac{3Q\sqrt{\gamma}\sinh(t/\sqrt{\gamma})}{(1 + Q\cosh(t/\sqrt{\gamma}))^2}, \\ v'(t) &= \frac{3Q(1/\sqrt{\gamma})\sinh(t/\sqrt{\gamma})}{(1 + Q\cosh(t/\sqrt{\gamma}))^2}. \end{aligned} \tag{4.6}$$

We plot u, v, and their derivatives in Figure 4.1.

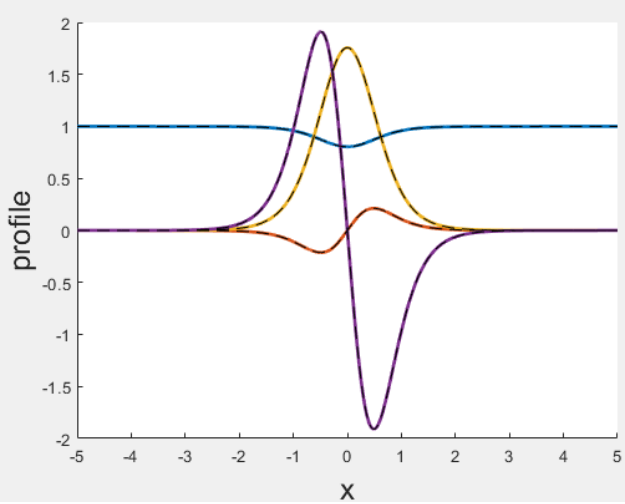

Figure 4.1: The graphs of the profile equations.

4.1.1 The eigenvalue problem. Linearizing (4.1) about the profile (4.5) and looking for separated solutions leads to the eigenvalue problem,

$$\begin{aligned} \lambda u &= u'' - u\hat{v}^2 - 2\hat{u}\hat{v}v - \alpha u, \\ \lambda v &= v'' + u\hat{v}^2/\gamma + 2\hat{u}\hat{v}v/\gamma - v/\gamma, \end{aligned} \tag{4.7}$$

where $\hat{u}$ and $\hat{v}$ are the profile solutions. Rearranging terms, we have

$$\begin{aligned} u'' &= \lambda u + \hat{v}^2 u + 2\hat{u}\hat{v}v + \alpha u, \\ v'' &= \lambda v - \frac{\hat{v}^2}{\gamma}u - \frac{2\hat{u}\hat{v}}{\gamma}v + \frac{v}{\gamma}. \end{aligned} \tag{4.8}$$

Note that, due to the symmetry of $\hat{u}$ and $\hat{v}$, eigenfunctions may be symmetric about the origin, or reflexive about the origin.

We write (4.8) as a first order system as follows,

$$\begin{pmatrix} u \\ u' \\ v \\ v' \end{pmatrix} = \begin{pmatrix} 0 & 1 & 0 & 0 \\ \lambda + \hat{v}^2 + \alpha & 0 & 2\hat{u}\hat{v} & 0 \\ 0 & 0 & 0 & 1 \\ -\hat{v}^2/\gamma & 0 & \lambda + (1 - 2\hat{u}\hat{v})/\gamma & 0 \end{pmatrix} \begin{pmatrix} u \\ u' \\ v \\ v' \end{pmatrix}. \tag{4.9}$$

The asymptotic matrices are given by

$$A_{\pm} = \begin{pmatrix} 0 & 1 & 0 & 0 \\ \lambda + \alpha & 0 & 0 & 0 \\ 0 & 0 & 0 & 1 \\ 0 & 0 & \lambda + 1/\gamma & 0 \end{pmatrix}. \tag{4.10}$$

The eigenvalues of $A_{\pm}$ are given by $\mu_1^{\pm} = \pm\sqrt{\lambda + \alpha}$ and $\mu_2^{\pm} = \pm\sqrt{\lambda + 1/\gamma}$. The associated eigenvectors are given by $v_1^{\pm} = (1, \mu_1^{\pm}, 0, 0)^T$ and $v_2^{\pm} = (0, 0, 1, \mu_2^{\pm})^T$. Thus, to compute the Evans function, we need to solve for the two-dimensional unstable manifold of (4.9) corresponding to $x = -\infty$, and for the two-dimensional stable manifold of (4.9) corresponding to $x = +\infty$. Even for computations using double arithmetic, this is an extremely challenging problem that requires specialized numerical solvers due to the conditioning of the problem; for example see [4, 20].

Rather than use specialized solvers, we may raise the dimension of the system using exterior products and solve for manifolds $W^{\pm\infty}(x; \lambda)$ of dimension one. An intersection of these one-dimensional manifolds in the larger system corresponds to an intersection of the two-dimensional manifolds in the original system. This method of using exterior products is known as the compound matrix method and is described in Section 2.3; for details see [1]. We note that in practice, the compound matrix method can only be used if the dimension of the system is sufficiently small since the dimension of the raised system can be much larger. We note that using the compound matrix method reduces the ODE problem we must solve

for the Gray-Scott equation to the same situation considered in Chapter 3. That is, we only need solve for a one-dimensional manifold.

The compound matrix corresponding to (4.9) is given by

$$B^{(2)} = \begin{pmatrix} 0 & 2\hat{u}\hat{v} & 0 & 0 & 0 & 0 \\ 0 & 0 & 1 & 1 & 0 & 0 \\ 0 & \lambda + (1 - 2\hat{u}\hat{v})/\gamma & 0 & 0 & 1 & 0 \\ 0 & \lambda + \hat{v}^2 + \alpha & 0 & 0 & 1 & 0 \\ \hat{v}^2/\gamma & 0 & \lambda + \hat{v}^2 + \alpha & \lambda + (1 - 2\hat{u}\hat{v})/\gamma & 0 & 2\hat{u}\hat{v} \\ 0 & \hat{v}^2/\gamma & 0 & 0 & 0 & 0 \end{pmatrix}.$$

The ODE to solve is then

$$W'_{\pm}(x) = B^{(2)}(x;\lambda)W_{\pm}(x), \tag{4.11}$$

where $W_+ : [0,\infty) \to \mathbb{R}^6$ belongs to the one-dimensional manifold of the fixed point zero of (4.11) corresponding to the eigenvalue of $B^{(2)}_+ := \lim_{x\to+\infty} B^{(2)}(x)$ with the most negative real part, and $W_- : (-\infty, 0] \to \mathbb{R}^6$ belongs to the unstable manifold of the fixed point zero of (4.11) corresponding to the eigenvalue of $B^{(2)}_- := \lim_{x\to-\infty} B^{(2)}(x)$ with the most positive real part. The Evans function is given by the inner product of $W_+(0)$ and $W_-(0)$.

At this point, we are ready to discuss the choice of μ in rescaling the Evans ODE.

4.2 Rescaling the Evans ODE

We discuss how to rescale the Evans ODE system (4.11) on the interval $(-\infty, 0]$. Rescaling on $[0, +\infty)$ follows an analogous procedure. We note that the eigenvalues of $B^{(2)}_-$ are given by the sum of the eigenvalues of A_-, and the corresponding eigenvectors of $B^{(2)}_-$ are given by the exterior products of the eigenvectors of A_-. We recall that the eigenvalues of A_- are given by $\pm\sqrt{\lambda+\alpha}$ and $\pm\sqrt{\lambda+1/\gamma}$. Thus, the eigenvalues of $B^{(2)}_-$ are given by

$$-\sqrt{\lambda+\alpha} - \sqrt{\lambda+1/\gamma}, \quad -\sqrt{\lambda+\alpha} + \sqrt{\lambda+1/\gamma}, \quad \sqrt{\lambda+\alpha} - \sqrt{\lambda+1/\gamma},$$
$$-\sqrt{\lambda+\alpha} + \sqrt{\lambda+\alpha} = 0, \quad -\sqrt{\lambda+1/\gamma} + \sqrt{\lambda+1/\gamma} = 0, \quad \sqrt{\lambda+\alpha} + \sqrt{\lambda+1/\gamma}.$$

The one dimensional manifold of the solution space of (4.11) that we wish to solve corresponds to eigenvalue $\mu_* := \sqrt{\lambda+\alpha} + \sqrt{\lambda+1/\gamma}$, the eigenvalue of $B_-^{(2)}$ with largest real part. If we rescale (4.11) so that $B^{(2)}(x;\lambda)$ goes to $B^{(2)}(x;\lambda) - \mu_* I$, then the solution we seek will converge at asymptotic rate to a non-zero multiple of the eigenvector corresponding to μ_*. However, this solution will belong to the center manifold of the fixed point zero of the rescaled system

$$W_\pm'(x) = (B^{(2)}(x;\lambda) - \mu I)W_\pm(x), \tag{4.12}$$

where $\mu = \mu_*$. We would not be able to obtain an analytic expansion of the desired manifold using the parameterization method because the solution we seek would not belong to the unstable manifold. We could instead choose $\mu = \mu_* - C$ where $C > 0$ is a constant that is small enough that the only eigenvalue of $B_-^{(2)} - \mu I$ that is greater than or equal to zero is $\mu_* - C$. We could then use the parameterization method to obtain an analytic basis for the unstable manifold of the ODE system obtained from coupling the profile ODE and (4.12) into one system. The unstable manifold of this coupled system would be three-dimensional. The unstable manifold of the profile is two-dimensional, and the unstable manifold of (4.12) is one dimensional with the choice $\mu = \mu_* - C$. However, we can do better than this. If we choose μ more carefully, we only need solve for a two-dimensional unstable manifold, which is easier to implement.

Recall that the eigenvalues of the Jacobian of the profile ODE at the fixed point corresponding to $x = -\infty$ are given by $\pm\sqrt{\alpha}$ and $\pm\sqrt{1/\gamma}$. Without loss of generality, assume that $\sqrt{1/\gamma} > \sqrt{\alpha}$. If we choose $\mu = \mu_* - \sqrt{\alpha}$, then only one eigenvalue, $\sqrt{\alpha}$, of $B_-^{(2)} - \mu I$ will have positive real part, and the eigenvector corresponding to $\sqrt{\alpha}$ will be the same eigenvector of $B_-^{(2)}$ that corresponds to the eigenvalue μ_*. Then the unstable manifold of the coupled system will be two-dimensional instead of three-dimensional. This is the same strategy we used for the system described in Chapter 3, only here the strategy is more involved since the profile has a two-dimensional unstable manifold.

We note that for $m, n \geq 0$, $m + n \geq 2$, if $m\sqrt{\alpha} + n\sqrt{1/\gamma}$ is an eigenvalue of $B_-^{(2)} - \mu I$,

or equals $\sqrt{\alpha}$ or $\sqrt{1/\gamma}$, then the recursion formula corresponding to the parameterization method is not solvable because the system is not invertible, something referred to as resonance. Our choice of μ, that is $\mu = \mu_* - \sqrt{\alpha}$, guarantees that the only possibility that $m\sqrt{\alpha} + n\sqrt{1/\gamma}$ is an eigenvalue of $B_-^{(2)} - \mu I$ is if $m\sqrt{\alpha} + n\sqrt{1/\gamma} = \sqrt{\alpha}$, but this can not happen for $m + n \geq 2$ since $\sqrt{\alpha} < \sqrt{1/\gamma}$ by assumption (without loss of generality). Thus, a resonance only arises in the computation of the unstable manifold for the Evans function if it does for the profile.

With this example of choosing the rescaling of the Evans ODE complete, we are almost ready to state our algorithm in its general form, but first we mention one other aspect of rigorous computation of the Evans function. We must obtain a bound on the region where unstable eigenvalues may occur. For the Gray-Scott system, we can do this with an energy estimate. For many systems, obtaining an energy estimate is much more difficult. For those systems, one may use other methods, but we propose that computer assisted proof can be used to make this process easier. First, we provide an energy estimate to bound the eigenvalues for the Gray-Scott system. Comparing this energy estimate to the one given in Section 3.5, we see how the level of difficulty already increases between these two systems. After providing the energy estimate, we present a strategy for using computer assisted proof to obtain a bound on the eigenvalues.

4.3 High frequency energy estimates

The eigenvalue problem is given by

$$\begin{aligned} \lambda u &= u'' - u\hat{v}^2 - 2\hat{u}\hat{v}v - \alpha u, \\ \lambda v &= v'' + u\hat{v}^2/\gamma + 2\hat{u}\hat{v}v/\gamma - v/\gamma, \end{aligned} \tag{4.13}$$

where $\hat{u}$ and $\hat{v}$ are the profiles.

Our goal is to obtain a bound on the region in the right-half complex plane where eigenvalues may occur. Using an energy estimate, we obtain the following result.

Theorem 14. *If λ is an eigenvalue of the ODE eigenvalue problem* (4.13) *and if* $\Re(\lambda) \geq 0$*, then*

$$|\Im(\lambda)| \leq \sqrt{\frac{2||\hat{v}||_\infty^3 ||\hat{u}||_\infty}{|\gamma|}}, \tag{4.14}$$

and

$$\Re(\lambda) \leq \max\left(||\hat{v}||_\infty^2 + 2||\hat{u}||_\infty ||\hat{v}||_\infty - \alpha, \frac{1}{|\gamma|}||\hat{v}||_\infty^2 + \frac{2}{|\gamma|}||\hat{u}||_\infty ||\hat{v}||_\infty - \frac{1}{\gamma} \right). \tag{4.15}$$

Proof. We multiply the first equation in (4.13) by $\bar{u}$ and the second equation in (4.13) by $\bar{v}$ where the bar indicates the complex conjugate, and then we integrate. We also use integration by parts on $\int u''\bar{u}$ and $\int v''\bar{v}$. This leads to

$$\begin{aligned} \lambda||u||^2 &= -||u'||^2 - \int \hat{v}^2|u|^2 - 2\int \hat{u}\hat{v}\bar{u}v - \alpha||u||^2, \\ \lambda||v||^2 &= -||v'||^2 + \frac{1}{\gamma}\int \hat{v}^2 u\bar{v} + \frac{2}{\gamma}\int \hat{u}\hat{v}|v|^2 - \frac{1}{\gamma}||v||^2. \end{aligned} \tag{4.16}$$

Taking the imaginary part of both sides, we have

$$\begin{aligned} \Im(\lambda)||u||^2 &= \Im\left(-2\int \hat{u}\hat{v}\bar{u}v\right), \\ \Im(\lambda)||v||^2 &= \Im\left(\frac{1}{\gamma}\int \hat{v}^2 u\bar{v}\right). \end{aligned} \tag{4.17}$$

Taking the absolute value of both sides and using standard bounds, we arrive at the inequalities

$$\begin{aligned} |\Im(\lambda)|||u||^2 &\leq 2||\hat{u}||_\infty ||\hat{v}||_\infty \int |\bar{u}v|, \\ |\Im(\lambda)|||v||^2 &\leq \frac{1}{|\gamma|}||\hat{v}^2||_\infty \int |u\bar{v}|. \end{aligned} \tag{4.18}$$

Multiplying the second equation above by $|\Im(\lambda)|$ and using the first inequality we find

$$|\Im(\lambda)|^2||v||_2 \leq \frac{2||\hat{v}||_\infty^3 ||\hat{u}||_\infty}{|\gamma|}||v||_2, \tag{4.19}$$

which implies that

$$|\Im(\lambda)| \leq \sqrt{\frac{2||\hat{v}||_\infty^3 ||\hat{u}||_\infty}{|\gamma|}}. \tag{4.20}$$

We now take the real part of both sides of (4.16) to obtain

$$\begin{aligned}\Re(\lambda)||u||_2^2 &= -||u'||_2^2 - \Re\left(\int \hat{v}^2|u|^2\right) - 2\Re\left(\int \hat{u}\hat{v}\bar{u}v\right) - \alpha||u||_2^2,\\ \Re(\lambda)||v||_2^2 &= -||v'||_2^2 + \frac{1}{\gamma}\int \hat{v}^2 u\bar{v} + \frac{2}{\gamma}\int \hat{u}\hat{v}|v|^2 - \frac{1}{\gamma}||v||^2.\end{aligned} \tag{4.21}$$

Bounding some terms on the right using standard techniques including Hölder's inequality leads to

$$\begin{aligned}\Re(\lambda)||u||_2^2 &\leq ||\hat{v}||_\infty^2||u||_2^2 + 2||\hat{u}||_\infty||\hat{v}||_\infty||u||_2||v||_2 - \alpha||u||_2^2,\\ \Re(\lambda)||v||_2^2 &\leq \frac{1}{|\gamma|}||\hat{v}||_\infty^2||u||_2||v||_2 + \frac{2}{|\gamma|}||\hat{u}||_\infty||\hat{v}||_\infty||v||_2^2 - \frac{1}{\gamma}||v||_2^2.\end{aligned} \tag{4.22}$$

We note that $||u||_2 > 0$ and $||v||_2 > 0$ if (u, v) forms an eigenfunction, so dividing the first equation above by $||u||_2^2$ if $||u||_2 > ||v||_2$, and dividing the second equation above by $||v||_2^2$ if $||v||_2 > ||u||_2$, we arrive at

$$\Re(\lambda) \leq \max\left(||\hat{v}||_\infty^2 + 2||\hat{u}||_\infty||\hat{v}||_\infty - \alpha, \frac{1}{|\gamma|}||\hat{v}||_\infty^2 + \frac{2}{|\gamma|}||\hat{u}||_\infty||\hat{v}||_\infty - \frac{1}{\gamma}\right). \tag{4.23}$$

□

This completes our proof on a bound on the region where unstable eigenvalues of (4.13) can exist, if there are any.

4.4 A strategy for obtaining bounds on unstable eigenvalues

In this section, we return to suggesting a strategy for bounding unstable eigenvalues using computer assisted proof. The Evans ODE often takes the form,

$$W' = A(x) + \lambda B(x).$$

Let $R = |\lambda|$ and rescale the Evans ODE to obtain

$$W' = \frac{1}{R}A(x) + \frac{\lambda}{R}B(x).$$

Now one can use rigorous computation to enclose the solution to this rescaled Evans ODE and show that for R sufficiently large, the manifold coming from the left and the right can not intersect.

We are now ready to summarize our algorithm for rigorous computation of the Evans function in its full generality.

Chapter 5. Summary

In this chapter, we summarize the algorithm that we presented in Chapters 3 and 4, and we discuss future directions.

5.1 The algorithm

We now summarize the algorithm that we presented in Chapters 3 and 4. The steps are as follows,

(i) Use the compound matrix method to lift the Evans ODE system.

(ii) Rescale the Evans ODE system so that the one dimensional manifold of the lifted Evans ODE system we wish to approximate corresponds to the eigenvalue of the Profile Jacobian at $x = -\infty$ with the smallest positive real part, or to the largest negative real part eigenvalue at $x = +\infty$.

(iii) Use the parameterization method to parameterize the unstable/stable manifold at $x = \mp\infty$ of the coupled profile and Evans ODE system.

(iv) Use a standard series solution to represent the solution to the coupled system over finite intervals.

(v) Form a zero-finding problem by forming a function F whose zero corresponds to a solution to the coupled ODE system.

(vi) Use the Newton-Kantorovich Theorem to obtain a bound on the error involved in our best approximation of the ODE solution.

(vii) Use analytic interpolation to interpolate the Evans function with rigorous error bounds.

In Chapter 3, we successfully demonstrated that this algorithm works for a diffusion equation. In Chapter 4, we showed how to deal with the case that the profile has a fixed point with a multi-dimensional stable/unstable manifold. This provides an algorithm for rigorously establishing spectral stability of traveling waves using the Evans function. For many systems, proving spectral stability is the last open problem in order to prove that traveling waves are stable.

5.2 Future directions

In this dissertation, we have developed a computer assisted method of proof for rigorously approximating the Evans function. This method enables proving spectral stability of traveling waves, the last open problem for proving stability of traveling waves for many physical systems. We have demonstrated this method for a scalar reaction-diffusion equation, and we have shown how to deal with more complicated cases as occur in the Gray-Scott equations we discussed in Chapter 4. The next step is to use this computer assisted method of proof to prove stability of traveling waves in physical models. This method would especially be helpful for proving stability of traveling waves in the compressible Navier-Stokes equation with a non-isentropic ideal gas equation of state and with a Van der Waal gas equation of state, and for the equations of magnetohydrodynamics with the same gas equations of state.

Appendix A. MATLAB Code

In this appendix, we provide our code for the scalar reaction-difusion system described in Chapter 3.

A.1 The driver

```
% scalar reaction-diffusion example
clear all; close all; beep off; clc; intvalinit('DisplayMidRad');

scale1 = 1;
scale2 = 1;
N = 30;

% solve for the Evans function non-rigorously and plot it
LAM = fliplr(linspace(1e-3,3,30));

D = zeros(size(LAM));

options = odeset('RelTol',1e-8,'AbsTol',1e-8);

for j = 1:length(LAM)


    lambda = LAM(j);
    mu_L = sqrt(1+lambda);
    mu_R = -sqrt(1+lambda);

    VL = [1;mu_L];
    VR = [1;mu_R];

    odefun_L = @(x,y)[-mu_L*y(1)+y(2);(mu_L^2-3*sech(x/2)^2)*y(1)-
        mu_L*y(2)];
```

```
26      odefun_R = @(x,y)[-mu_R*y(1)+y(2);(mu_R^2-3*sech(x/2)^2)*y(1)-
            mu_R*y(2)];
27
28      sol_L = ode15s(odefun_L,[-15,0],VL,options);
29      sol_R = ode15s(odefun_R,[15,0],VR,options);
30
31
32      temp_L = deval(sol_L,0);
33      temp_R = deval(sol_R,0);
34
35      D(j) = temp_L(1)*temp_L(2);
36
37  end
38
39  % figure;
40  plot(LAM,D,'-k','LineWidth',2);
41  h = xlabel('\lambda');
42  set(h,'FontSize',18);
43  h = ylabel('D(\lambda)');
44  set(h,'FontSize',18);
45  h = gca;
46  set(h,'FontSize',18);
47
48  %
```

```
49  % Obtain a bound on the Evans function ODE manifolds
```

```
50 %
   ------------------------------------------------------------------------

51
52 % obtain the left and right side of the interval of mu values for
       our Evans
53 % function comptuation
54 lambda_left = iv(0);
55 lambda_right = iv(2);
56 mu_left = sqrt(1+lambda_left)-1;
57 mu_right = sqrt(1+lambda_right)-1;
58
59 % Choose rho for the stadium for getting the bound on
       interpolation of the
60 % Evans function ODE manifolds. The coefficients of the left
       manifold are
61 % analytic if the real part of mu is greater than -0.5.
62 rho_mu = 3;
63
64 % compute the manifold at infinity
65 d = manifold_at_infty(0);
66
67 % choose the finit evalue of x where the left manifold meets the
       middle
68 % manifold
69 x_L = -5;
70
```

```
71 % get the value of the profile at x = x_L
72 y_L = 1.5*sech(x_L/2)^2;
73
74 % Determine which value of theta corresponds to the manifold
       connecting to
75 % the profile
76 fun = @(theta) mid([1,0]*eval_manifold_at_infty(d.y_n,d.z_n,theta
       ,0)-y_L);
77
78 options = optimset('Display','off', 'Jacobian','off', ...
79           'Algorithm','Levenberg-Marquardt','TolFun',1e-8);
80
81 [theta_L,res_err,success] = fsolve(fun,0.01,options);
82
83 % Get the stadium for analytic interpolation
84 theta = linspace(0,sup(2*iv('pi')),11);
85 theta = iv(theta(1:end-1),theta(2:end));
86
87 mu_tilde = (rho_mu*exp(1i*theta)+1./(rho_mu*exp(1i*theta)))/2;
88 mu = (mu_left+mu_right)/2+(mu_right-mu_left)*mu_tilde/2;
89
90 min(inf(real(mu)))
91 if min(inf(real(mu))) <= -1/2
92     error('Real(mu) > -0.5 required for the coefficients to be
          analytic');
93 end
94
```

```
% Find a bound for the analytic interpolation error bound
M_rho = 1;
max_C0 = 0; % Also, find the max of C0 and C
max_C = 0;
for j = 1:length(theta)

    d = manifold_at_infty(mu(j));

    C0 = max(sup(abs([1,d.y_n(1),d.z_n(1),d.v_n(1),d.w_n(1)])));
    C = 0;
    for k = 2:length(d.y_n)
        temp = [(d.y_n(k)/C0)^(1/(k-1)),(d.z_n(k)/C0)^(1/(k-1)),
            ...
            (d.v_n(k)/C0)^(1/(k-1)),(d.w_n(k)/C0)^(1/(k-1))];
        C = max([C,max(sup(abs(temp)))]);
    end

    max_C0 = max([C0,max_C0]);
    max_C = max([C,max_C]);

    VL = eval_manifold_at_infty(d.v_n,d.w_n,theta_L,d.C);
    M_rho = max(M_rho,max(sup(norm(VL))));

end

max_mu = iv(max(sup(abs(mu))));
max_lam = iv(max(sup(abs((mu+1).^2-1))));
```

```
operator_bound = sqrt(24+2*max_mu^2+6*max_lam+max_lam^2);

% the number of nodes needed to track just one component of Evans
    product.
M_rho = M_rho*exp(abs(x_L)*operator_bound);

% find out how many Chebyshev nodes are needed for the desired
    error bound
pie = iv('pi');
D_rho = (rho_mu+1/rho_mu)/2-1;
L_rho = pie*sqrt(rho_mu^2+1/rho_mu^2);

M = 1;
eta = log(rho_mu);
interpolation_error = 10^5;
while sup(interpolation_error) > 1e-10
    M = M+1;
    interpolation_error = M_rho*L_rho/(pie*D_rho*sinh(eta*(M+1)));
end
M

%
```

```
% Evans function using the re-scaled manifold
%
```

```
143
144 ode_options = odeset('RelTol',1e-8,'AbsTol',1e-8);
145
146 theta = (2*iv(0:1:M-1)+1)*pie/(2*M);
147 mu_tilde = cos(theta);
148 mu = (mu_left+mu_right)/2+(mu_right-mu_left)*mu_tilde/2;
149 LAM = (mu+1).^2-1;
150 D = iv(zeros(1,length(LAM)));
151
152 disp('Computing the Evans function');
153 figure;
154 hold on;
155 h = xlabel('\lambda');
156 set(h,'FontSize',18);
157 h = ylabel('D(\lambda)');
158 set(h,'FontSize',18);
159 h = gca;
160 set(h,'FontSize',18);
161 t_start = tic;
162 for j = 1:length(LAM)
163     j
164     lambda = LAM(j);
165
166     mu_L = sqrt(1+lambda)-1;
167
168     D(j) = NK(mu_L,theta_L,x_L);
```

```
169
170         Dlam = D(j);
171
172         plot(mid(lambda),mid(D(j)),'.k','MarkerSize',18);
173         drawnow;
174
175
176
177 end
178 evans_run_time = toc(t_start);
179
180
181 figure;
182 plot(LAM,mid(D),'-b','LineWidth',2);
183 h = xlabel('\lambda');
184 set(h,'FontSize',18);
185 h = ylabel('D(\lambda)');
186 set(h,'FontSize',18);
187 h = gca;
188 set(h,'FontSize',18);
```

A.2 Evaluation of the unstable manifold

```
1 function [out,out_der,out_der_der] = eval_manifold_at_infty(A_n,
      B_n,theta,C)
2
3 % sum the finite number of terms
4 out = zeros(2,1);
```

```
for n = fliplr(0:length(A_n)-1)
    out = out + theta^n*[A_n(n+1);B_n(n+1)];
end

% sum the finite number of terms in derivative
out_der = zeros(2,1);
for n = fliplr(1:length(A_n)-1)
    out_der = out_der + n*theta^(n-1)*[A_n(n+1);B_n(n+1)];
end

% sum the finite number of terms in second derivative
out_der_der = zeros(2,1);
for n = fliplr(2:length(A_n)-1)
    out_der_der = out_der_der + n*(n-1)*theta^(n-2)*[A_n(n+1);B_n(
        n+1)];
end

% Get a bound on the tale of the dominating geometric series
r = abs(C*theta/2);
if  sup(r) >= 1
   error('0<r<1 required');
end

% Add the truncation error bound
N = length(A_n)-1;
f = r^(N+1)/(1-r)/2;
out = out + iv(-f,f);
```

```
31
32 f_der = ((N+1)*r^N/(1-r)+r^(N+1)/(1-r)^2)/2;
33 out_der = out_der + iv(f_der*C/4,-f_der*C/4);
34
35
36 temp1 = (N+1)*N*r^(N-1)/(1-r);
37 temp2 = 2*(N+1)*r^N/(1-r)^2;
38 temp3 = r^(N+1)/(1-r)^3;
39 f_der_der = (temp1+temp2+temp3)/2;
40 out_der_der = out_der_der+iv(f_der_der*C^2/8,-f_der_der*C^2/8);
```

A.3 The interval

```
1 function out = iv(num1,num2)
2 % function out = iv(num)
3 %
4 % returns a mathematically rigorous enclosure of the number of
     interval
5 % given.
6
7 if nargin == 1
8     out = intval(num1);
9 elseif nargin == 2
10     out = hull(intval(num1),intval(num2));
11 end
```

A.4 Obtaining the unstable manifold

```
1 function d = manifold_at_infty(mu)
```

```
2
3 %{
4       mu = sqrt(1+lambda)-1;
5 %}
6
7 t_start = tic;
8
9 % N = 20 suffices yeilds the desired error bound (0 \leq mu \leq
      1)
10 N = 20;
11
12 % initialize the coefficients
13 y_n = iv(zeros(N+1,1));
14 z_n = iv(zeros(N+1,1));
15 v_n = iv(zeros(N+1,1));
16 w_n = iv(zeros(N+1,1));
17
18 % Record the eigenvector corresponding to eigenvalue 1
19 y_n(2) = 1;
20 z_n(2) = 1;
21 v_n(2) = 1;
22 w_n(2) = 1+mu;
23
24 % define C as needed for the proposition
25 C = iv(4*max(sup([1,abs(1+mu)])));
26
27 % Compute the coefficients
```

```
28 for n = 2:N
29
30     % sum that shows up in the RHS
31     sm1 = y_n(2:n).'*flipud(y_n(2:n));
32
33     % Solve for the first two components
34     temp = ([n 1; 1 n]*[0;-sm1])/(n^2-1);
35
36     % Record the coefficients
37     y_n(n+1) = temp(1);
38     z_n(n+1) = temp(2);
39
40     % sum that shows up in the RHS of the last two components
41     sm2 = y_n(2:n).'*flipud(v_n(2:n));
42
43     % Solve for the last two components
44     temp = ([n+mu,1; (mu+1)^2, n+mu]*[0;-2*sm2])/((n+mu)^2-(mu+1)
           ^2);
45
46     v_n(n+1) = temp(1);
47     w_n(n+1) = temp(2);
48
49 end
50
51 % record C
52 d.C = C;
53
```

```
54 % record the coefficients
55 d.y_n = y_n;
56 d.z_n = z_n;
57 d.v_n = v_n;
58 d.w_n = w_n;
59
60 % record the run time for this function
61 d.run_time = toc(t_start);
```

A.5 The series solutions on finite intervals

```
1  function d = middle_rig(U0,delx,mu,N)
2
3  d.mu = mu;
4  d.N = N;
5  d.delx = delx;
6  d.U0 = U0;
7
8  t_start = tic;
9
10 m = 1;
11
12 % initialize coefficients
13 Q = iv(zeros(4,N+1));
14 DQ = iv(zeros(4,4,N+1));
15 D2Q = iv(zeros(4,4,4,N+1));
16
17 Q(:,1) = U0;
```

```
18
19 DQ(:,:,1) = eye(4);
20
21 % obtain $C_0$
22 temp1 = max(sup(abs(Q(:,1))));
23 temp2 = max(max(sup(abs(DQ(:,:,1)))));
24 temp3 = max(max(max(sup(abs(D2Q(:,:,:,1))))));
25
26 C0 = 2^m*iv(max([temp1,temp2,temp3]));
27
28 C = 0;
29 for n = 0:N
30
31     % sum(y_n-k * y_k)
32     sm1 = newconvolution(squeeze(Q(1,:)),squeeze(Q(1,:)),n);
33
34     % sum(y_n-k * v_k)
35     sm2 = newconvolution(squeeze(Q(1,:)),squeeze(Q(3,:)),n);
36
37     % sum(Dy_{n-k} * y_k + y_{n-k} * Dy_k)
38     sm3 = iv([0,0,0,0]);
39     for i = 1:4
40         sm3(1,i) = newconvolutionbig(squeeze(DQ(1,i,:)),squeeze(Q
               (1,:)),n) ...
41             + newconvolutionbig(squeeze(Q(1,:)),squeeze(DQ(1,i,:))
                   ,n);
42     end
```

```
43
44      % sum(Dy_k * v_{n-k} + y_k * Dv_{n-k})
45      sm4 = iv([0,0,0,0]);
46      for i = 1:4
47          sm4(1,i) = newconvolutionbig(squeeze(DQ(1,i,:)),squeeze(Q
                (3,:)),n) ...
48              + newconvolutionbig(squeeze(Q(1,:)),squeeze(DQ(3,i,:))
                    ,n);
49      end
50
51      % sum(D2y_{n-k} * y_k + y_{n-k} * D2y_k + 2 Dy_{n-k} * Dy_k)
52      sm5 = iv(zeros(4,4));
53      for i = 1:4
54          for k = 1:4
55              sm5(1,i,k) = newconvolutionbig(squeeze(D2Q(1,i,k,:)),
                    squeeze(Q(1,:)),n) + ...
56                  newconvolutionbig(squeeze(Q(1,:)),squeeze(D2Q(1,i,
                        k,:)),n) ...
57                  + 2*newconvolutionbig(squeeze(DQ(1,i,:)),squeeze(
                        DQ(1,i,:)),n);
58          end
59      end
60
61      % sum(D2y_n-k * v_k + y_n-k * D2v_k + 2 Dy_n-k * Dv_k)
62      sm6 = iv(zeros(4,4));
63      for i = 1:4
64          for k = 1:4
```

```
65              sm6(1,i,k) = newconvolutionbig(squeeze(D2Q(1,i,k,:)),
                    squeeze(Q(3,:)),n) ...
66                  + newconvolutionbig(squeeze(Q(1,:)),squeeze(D2Q(3,
                        i,k,:)),n) + ...
67                  2*newconvolutionbig(squeeze(DQ(1,i,:)),squeeze(DQ
                        (3,i,:)),n);
68          end
69      end
70
71      Q(1,n+2) = Q(2,n+1)/(n+1);
72      Q(2,n+2) = (Q(1,n+1)-sm1)/(n+1);
73      Q(3,n+2) = (Q(4,n+1)-mu*Q(3,n+1))/(n+1);
74      Q(4,n+2) = ((mu+1)^2*Q(3,n+1)-mu*Q(4,n+1)-2*sm2)/(n+1);
75
76      for k = 1:4
77          DQ(1,k,n+2) = DQ(2,k,n+1)/(n+1);
78          DQ(2,k,n+2) = (DQ(1,k,n+1)-sm3(k))/(n+1);
79          DQ(3,k,n+2) = (DQ(4,k,n+1)-mu*DQ(3,k,n+1))/(n+1);
80          DQ(4,k,n+2) = ((mu+1)^2*DQ(3,k,n+1)-mu*DQ(4,k,n+1)-2*sm4(k
                ))/(n+1);
81      end
82
83      for k = 1:4
84          for j = 1:4
85              D2Q(1,k,j,n+2) = D2Q(2,k,j,n+1)/(n+1);
86              D2Q(2,k,j,n+2) = (D2Q(1,k,j,n+1)-sm5(k,j))/(n+1);
87              D2Q(3,k,j,n+2) = (D2Q(4,k,j,n+1)-mu*D2Q(3,k,j,n+1))/(n
```

```
                +1);
88              D2Q(4,k,j,n+2) = ((mu+1)^2*D2Q(3,k,j,n+1)-mu*D2Q(4,k,j,
                    n+1) ...
89                    -2*sm6(k,j))/(n+1);
90          end
91      end
92
93      temp1 = max(sup(abs(Q(:,n+2))));
94      temp2 = max(max(sup(abs(DQ(:,:,n+2)))));
95      temp3 = max(max(max(sup(abs(D2Q(:,:,:,n+2))))));
96
97      maxabs = 2^m*iv(max([temp1,temp2,temp3]));
98
99      if  n > 0
100         C = max(C,sup((maxabs/C0)^(iv(1)/n)));
101     end
102
103 end
104 C = iv(C);
105
106 out = iv(zeros(4,1));
107 for n = fliplr(0:N)
108     out = out + Q(:,n+1)*delx^n;
109 end
110
111 out_der = iv(zeros(4,4));
112 for n = fliplr(0:N)
```

```
113     out_der = out_der + DQ(:,:,n+1)*delx^n;
114 end
115
116 out_der_der = iv(zeros(4,4,4));
117 for n = fliplr(0:N)
118     out_der_der = out_der_der + D2Q(:,:,:,n+1)*delx^n;
119 end
120
121 r = abs(C*delx);
122 if sup(r)>= 1
123     error('bounds are not valid');
124 end
125 err_bound = C0*r^(N+1)/(1-r);
126
127 err = 2^(-m)*iv(-err_bound,err_bound);
128
129 d.C0 = C0;
130 d.C = C;
131
132 d.U = out + err;
133 d.DU = out_der + err;
134 d.D2U = out_der_der+err;
135
136 d.err = err;
137 d.r = r;
138
139 d.run_time = toc(t_start);
```

A.6 The convolution of vectors

```
function out = newconvolutionbig(u,w,n)
% convolution of u(1:n) and w(1:n)

u=squeeze(u);
w=squeeze(w);

if size(u,2) < size(u,1)
    u=u.';
end

if size(w,1) < size(w,2)
    w=w.';
end

out = u(1:n)*flipud(w(1:n));
```

A.7 The Newton-Kantorovich Theorem

```
function D = NK(mu,theta_L,x_L)

delx = 0.1; % step size

r_newton = 1e-5; % goal is to show error is no bigger than this

ode_options = odeset('RelTol',1e-14,'AbsTol',1e-14);

```

```
% get the parameterization of unstable manifold at x = -infty
dinf = manifold_at_infty(mu);

% evaluate the unstable manifold at $\theta_L$
VL = eval_manifold_at_infty(dinf.v_n,dinf.w_n,theta_L,dinf.C);

% Solve the Evans ODE non-rigorously
mud = mid(mu);
odefun_L = @(x,y)[-mud*y(1)+y(2);((mud+1)^2-3*sech(x/2)^2)*y(1)-
    mud*y(2)];
sol_L = ode15s(odefun_L,[x_L,0],mid(VL),ode_options);

% form $\bar x$, the guess at the solution to $F$ for the
% Newton-Kantorovich method
dom_bar = x_L:delx:0;
evans_bar = deval(sol_L,dom_bar);
prof_bar = [1.5*sech(dom_bar/2).^2; -1.5*sech(dom_bar/2).^2.*tanh(
    dom_bar/2)];


N = 4*length(dom_bar)+1; % number of equations

% instantiate $F$ and its derivative $DF$
F = iv(zeros(N,1));
DF = iv(zeros(N,N));

% equations 1-4 regarding variable theta_L
```

```
34 [pf1,pf2,pf3] =  eval_manifold_at_infty(dinf.y_n,dinf.z_n,theta_L,
       dinf.C);
35 [ef1,ef2,ef3] =  eval_manifold_at_infty(dinf.v_n,dinf.w_n,theta_L,
       dinf.C);
36
37 % The first four equations require the manifold coming from x = -
       infty
38 % to match the ODE solution at $x_0$
39 F(1:2) = pf1-prof_bar(:,1);
40 F(3:4) = ef1-evans_bar(:,1);
41
42 DF(1:2,1) = pf2;
43 DF(3:4,1) = ef2;
44 DF(1:4,2:5) = -eye(4);
45
46 % Now compute the series solution at the nodes $x_1, x_2, ...,
       x_n$
47 dm{length(dom_bar)-1}=[];
48 dmr{length(dom_bar)-1}=[];
49 r_int = iv(-r_newton,r_newton);
50 for j = 1:length(dom_bar)-1
51
52     dm{j} = middle_rig([prof_bar(:,j);evans_bar(:,j)],delx,mu,35);
53     dmr{j} = middle_rig([prof_bar(:,j)+r_int;evans_bar(:,j)+r_int
           ],delx,mu,25);
54
55 end
```

```
56
57 % Now use the series solutions on the finite inetervals $[x_j,x_{j
       +1}]$, to
58 % fill out $F$ and $DF$, and to get a bound on $D_2F$.
59 B = max(sup(abs([pf3;ef3])));
60 Id = iv(eye(4));
61 for j = 1:length(dom_bar)-1
62
63     d = dm{j};
64     dr = dmr{j};
65     F(4*j+1:4*j+4) = d.U-[prof_bar(:,j+1);evans_bar(:,j+1)];
66
67     DF(4*j+1:4*j+4,4*(j-1)+2:4*j+1) = d.DU;
68     DF(4*j+1:4*j+4,4*j+2:4*(j+1)+1) = -Id;
69
70     B1 = max(max(max(sup(abs(dr.D2U)))));
71     B = max([B,B1]);
72
73 end
74 B = iv(B);
75
76 % Finally, fill out $F$ and $DF$ for the last equation which has
       to do with
77 % the derivative of the profile being zero at $x = 0$
78 F(end) = prof_bar(2,end);
79 DF(end,end-2) = 1;
80
```

```
% Choose $A_{dagger}$ and $A$ and get the bounds needed for the
% Newton-Kantorovich Theorem.
J = mid(DF);

A_dagger = iv(J);
A = iv(J\eye(size(J,1)));

Y0 = norm(A*F);
Id = eye(size(A,1));
Z0 = norm(Id-A*A_dagger,'fro');
Z1 = norm(A*(A_dagger-DF));
Z2r = norm(A,2)*norm(iv(-B,B)*ones(size(A)));

% Now show that the polynomial evaluates to be negative for r_newt
    ,
% which guarantees the error is no bigger than r_newt
r_newt = 5e-9;
newton_kantorovich_poly = Z2r*r_newt^2-(1-Z0-Z1)*r_newt+Y0;

if sup(newton_kantorovich_poly) >= 0
    error('Failed to verify the solution');
end

% add on error bound to Evans function computation
err = iv(-r_newt,r_newt);

D =  (evans_bar(1,end)+err)*(evans_bar(2,end)+err);
```

Bibliography

[1] Leanne Allen and Thomas J. Bridges. Numerical exterior algebra and the compound matrix method. *Numerische Mathematik*, 92(2):197–232, Aug 2002.

[2] Gianni Arioli and Hans Koch. Some breathers and multi-breathers for FPU-type chains. *Communications in Mathematical Physics*, 372(3):1117–1146, Mar 2019.

[3] Blake Barker. Numerical proof of stability of roll waves in the small-amplitude limit for inclined thin film flow. *Journal of Differential Equations*, 257(8):2950–2983, Oct 2014.

[4] Blake Barker, Rose Nguyen, Björn Sandstede, Nathaniel Ventura, and Colin Wahl. Computing evans functions numerically via boundary-value problems. *Physica D: Nonlinear Phenomena*, 367:1–10, Mar 2018.

[5] Blake Barker and Kevin Zumbrun. Numerical proof of stability of viscous shock profiles. *Mathematical Models and Methods in Applied Sciences*, pages 1–19, Sep 2016.

[6] Blake H. Barker. *Evans Function Computation*. BYU Scholars Archive, 2009.

[7] Margaret Beck and Jonathan Jaquette. Validated spectral stability via conjugate points. *SIAM Journal on Applied Dynamical Systems*, 21(1):366–404, 2022.

[8] Jan Bouwe van den Berg and Jean-Philippe Lessard. *Rigorous Numerics in Dynamics*. American Mathematical Society, 2016.

[9] Fred Brauer. Bounds for solutions of ordinary differential equations. *Proceedings of the American Mathematical Society*, 14(1):36–43, Feb. 1963.

[10] Leon Q. Brin. Numerical testing of the stability of viscous shock waves. *Math. Comp.*, 70(235):1071–1088, 2001.

[11] R. Conti. Sulla prolugabilita delle soluzioni di un sistema di equazioni differenziali ordinarie. *Boll. Un. Math. Ital.*, 11:510–514, 1956.

[12] Arjen Doelman, Björn Sandstede, Arnd Scheel, and Guido Schneider. The dynamics of modulated wave trains. *Mem. Amer. Math. Soc.*, 199(934), 2009.

[13] Javier Gómez-Serrano. Computer-assisted proofs in PDE: a survey. *SeMA Journal*, 76(3):459–484, February 2019.

[14] Jonathan Goodman. Nonlinear asymptotic stability of viscous shock profiles for conservation laws. *Arch. Rational Mech. Anal.*, 1986.

[15] Manoussos Grillakis, Jalal Shatah, and Walter Strauss. Stability theory of solitary waves in the presence of symmetry. *Journal of Functional Analysis*, 74(1):160–197, Sep 1987.

[16] Olivier Guès, Guy Métivier, Mark Williams, and Kevin Zumbrun. Existence and stability of multidimensional shock fronts in the vanishing viscosity limit. *Archive for Rational Mechanics and Analysis*, 175(2):151–244, Nov 2004.

[17] J. K. Hale, L. A. Peletier, and W. C. Troy. Exact homoclinic and heteroclinic solutions of the Gray-Scott model for autocatalysis. *SIAM Journal on Applied Mathematics*, 61(1):102–130, 2000.

[18] Daniel Henry. *Geometric Theory of Semilinear Parabolic Equations*, volume 840. Springer Berlin Heidelberg, 1981.

[19] Peter Howard and Kevin Zumbrun. Pointwise estimates and stability for dispersive–diffusive shock waves. *Archive for Rational Mechanics and Analysis*, 155:85–169, 11 2000.

[20] Jeffrey Humpherys and Kevin Zumbrun. An efficient shooting algorithm for Evans function calculations in large systems. *Phys. D*, 220(2):116–126, 2006.

[21] Mathew A. Johnson, Pascal Noble, L. Miguel Rodriguez, and Kevin Zumbrun. Behaviour of periodic solutions of viscous conservation laws under localized and nonlocalized perturbations. *Inventiones mathematicae*, 197(1):115–213, 2014.

[22] Serge Lang. *Complex Analysis*. Springer, 1998.

[23] Veerle Ledoux, Simon J. A. Malham, and Vera Thümmler. Grassmannian spectral shooting. *Math. Comp.*, 79(271):1585–1619, Jan 2010.

[24] Jean-Philippe Lessard and J. D. Mireles James. Computer assisted fourier analysis in sequence spaces of varying regularity. *SIAM Journal on Mathematical Analysis*, 49(1):530–561, January 2017.

[25] Tai-Ping Liu. Nonlinear stability of shock waves for viscous conservation laws. *Mem. Amer. Math. Soc.*, 56, 1985.

[26] Tai-Ping Liu. Pointwise convergence to shock waves for viscous conservation laws. *Communications on Pure and Applied Mathematics*, 50(11):1113–1182, 1997.

[27] Corrado Mascia and Kevin Zumbrun. Stability of viscous shock profiles for dissipative symmetric hyperbolic-parabolic systems, 2001.

[28] Corrado Mascia and Kevin Zumbrun. Pointwise Green function bounds for shock profiles of systems with real viscosity. *Arch. Ration. Mech. Anal.*, 169(3):177–263, 2003.

[29] Corrado Mascia and Kevin Zumbrun. Stability of large-amplitude viscous shock profiles of hyperbolic-parabolic systems. *Arch. Ration. Mech. Anal.*, 172(1):93–131, 2004.

[30] Akitaka Matsumura and Kenji Nishihara. On the stability of travelling wave solutions of a one-dimensional model system for compressible viscous gas. *Japan Journal of Applied Mathematics*, 2:17–25, 1985.

[31] Mitsuhiro T. Nakao, Michael Plum, and Yoshitaka Watanabe. *Numerical Verification Methods and Computer-Assisted Proofs for Partial Differential Equations*. Springer, 2019.

[32] S. C. Reddy and J. A. C. Weideman. The accuracy of the Chebyshev differencing method for analytic functions. *Siam Journal on Numerical Analysis*, 42(5):2176–2184, 2005.

[33] S.M. Rump. INTLAB - INTerval LABoratory. In Tibor Csendes, editor, *Developments in Reliable Computing*, pages 77–104. Kluwer Academic Publishers, Dordrecht, 1999.

[34] Björn Sandstede, Arnd Scheel, Guido Schneider, and Hannes Uecker. Diffusive mixing of periodic wave trains in reaction-diffusion systems. *J. Diff. Eq.*, 252(5):3541–3574, 2012.

[35] D. H. Sattinger. On the stability of waves of nonlinear parabolic systems. *Advances in Math.*, 22(3):312–355, 1976.

[36] Anders Szepessy and Zhouping Xin. Nonlinear stability of viscous shock waves. *Arch. Rational Mech. Anal.*, 122, 1993.

[37] Eitan Tadmor. The exponential accuracy of fourier and chebyshev differencing methods. *SIAM Journal on Numerical Analysis*, 23(1):1–10, 1986.

[38] Warwick Tucker. *Validated Numerics: A Short Introduction to Rigorous Computations*. Princeton University Press, 2011.

[39] J. B. van den Berg and J. D. Mireles James. Parameterization of slow-stable manifolds and their invariant vector bundles: Theory and numerical implementation. *Discrete and Continuous Dynamical Systems*, 36(9):4637–4664, 2016.

[40] A. Wintner. Ordinary differential equations and laplace transforms. *Amer. J. Math.*, 79:265–294, 1957.

[41] Kevin Zumbrun. Planar stability criteria for viscous shock waves of systems with real viscosity. In *Hyperbolic systems of balance laws*, volume 1911 of *Lecture Notes in Math.*, pages 229–326. Springer, Berlin, 2007.

[42] Kevin Zumbrun and Peter Howard. Pointwise semigroup methods and stability of viscous shock waves. *Indiana Univ. Math. J.*, 47(3):741–871, 1998.